Investigationon Groundwater Recharge Mapping Using GIS based intgarted spatial sdeceion making systesms A Case Study from Quetta Region, Pakistan

Imad Ali[1]*, Maryam Byati khatibi[2], Sadra Karimzadeh[3]

1. Ph. D. Student, Department of Remote Sensing and GIS, University of Tabriz, Tabriz, Iran. imadali_khan@yahoo.com
2. Professor, Department of Remote Sensing and GIS, University of Tabriz, Tabriz, Iran. m_bayati@tabrizu.ac.ir
3. Ascociate professor, Department of Remote Sensing and GIS, University of Tabriz, Tabriz, Iran. skharimzadeh@tabrizu.ac.ir

Keywords

Groundwater recharges zoning; Analytical hierarchy process; Integrated-Analytical hierarchy process; Frequency ratio; Quetta region;Pakistan.

Received: 2024/04/20

Accepted: 2024/06/24

Published: 2024/10/21

ABSTRACT

Groundwater is an essential resource in arid and semi-arid regions, where water scarcity and droughts are common. The Quetta region of Pakistan is one such area that requires effective groundwater recharge zone mapping to manage groundwater resources adequately. This study aimed to delineate groundwater recharge zones using a combination of analytical hierarchy process (AHP), fuzzy-AHP, and frequency ratio (FR) models. Additionally, it aimed to compare the effectiveness of these models in groundwater recharge potential zone mapping. To achieve these objectives, nine groundwater influencing factors were considered, including geology, soil types, lineament density, elevation, slope, topographic wetness index, drainage density, land use land cover, and rainfall. Thematic maps for all these factors were generated using satellite and conventional data in the ArcGIS environment. Weight was assigned to each thematic layer based on its significance to recharge. All thematic layers were combined using AHP model-l (WLC), AHP model-ll (Weighted sum), fuzzy-AHP overlay, and FR-based model using ArcGIS. The findings revealed that 15% and 39% of the study area have high recharge potentials according to AHP-based model-l and model-ll, respectively. The FAHP model demarcated 43% of the area as high recharge zones while the FR model demarcated 42% of the area as high recharge zones. The majority of high groundwater recharge areas were found in the central part of the study area, while the southern part was demarcated as a moderate recharge zone. The eastern and western parts were demarcated as low recharge potentials zones. To validate the accuracy of these models, the study used receiver operating characteristic (ROC) validation curves. The ROC curves revealed that AHP model-ll had the highest accuracy (AUC=89%) followed by the FAHP model (AUC=88%), AHP model-l (AUC=84%), and FR (AUC=81%). In conclusion, AHP model-ll was shown to be more effective in recharge zone demarcation compared to FAHP and FR models in the current study. The results of this study can benefit decision-makers in GW resource management and future planning in land use for urban extension, particularly in water-scarce regions of the country. Moreover, it can assist in the installation of future boreholes or dug/tube wells in the study area, which can minimize the cost and effort of hydrogeological investigation. This study's findings can provide valuable insights to professionals, researchers, and policymakers working in groundwater resource management.

* Corresponding Author: Imad Ali
E-mail: imadali_khan@yahoo.com

How cite to this article: Imad Ali, Maryam Byati khatibi, Sadra Karimzadeh (2024). A Comparative Study of Groundwater Recharge Mapping Using GIS based intgarted spatial sdeceion making systesms: A Case Study from Quetta Region, Pakistan. Hydrogeomorphology, 11(40): 58 – 86.

DOI: 10.22034/hyd.2024.61290.1734

 Publisher: University of Tabriz

Water is known as critical source of life indeed. Certainly, population evolution, aging infrastructure, climate change, and an upsurge in strict water quality standards are the main aspects that evidence it (Chandra, 2006; Selvam et al., 2014). Despite its importance, water is a poorly managed natural resource on the earth's planet (Miller & Spoolman, 2007). Groundwater (GW) is a type of water present in subsurface fractured lithological formations and soil pores (Gebrie et al., 2018). In both developed and developing countries worldwide, GW has emerged as a vital and reliable source of water for both urban and rural areas (Todd & Mays, 2004). GW is the foremost source of water for irrigation and agricultural activities worldwide. It is worth noting that more than 60% of agricultural practices are dependent on GW (Thakur et al., 2018).

Pakistan ranks fourth in the world in terms of the amount of GW extracted for irrigation purposes. Only 27% of the entire area is irrigated by surface water supplies, while the remaining 73% depends on GW either directly or indirectly. Presently, around 1.2 million private tube wells abstracting GW in the country, having an annual abstraction rate of around 65 billion cubic meters (Qureshi, 2020). Baluchistan province is situated in an arid to semi-arid climatic zone of Pakistan. In this area, the source of surface water is non-perennial, which means that GW is the only dependable source for municipal, industrial, and agricultural usage (Abdul S. Khan & Khan, 2013; Abdul S Khan et al., 2013; Mondal & Dalai, 2017; Watto, 2015). Agriculture is the key pillar of the economy of about 85% population of the province (Ashraf et al., 2014). The province was hit by numerous severe droughts in history, which had a radical influence on livelihoods and its economy and destroyed around 80% of its fruit orchids(Ashraf & Routray, 2015).Over 40% of the population of the province resides in the Pishin basin, with most living in and around the Quetta region (study area). Over the course of the last decade, the population of the Quetta region has experienced a significant increase from 1.02 million to 1.8 million individuals. The escalation of population density has been observed to correlate with a subsequent surge in the demand for agricultural and industrial water, ultimately leading to an exacerbation of water scarcity in the study area. This phenomenon highlights a significant challenge that needs to be addressed, as it poses a serious threat to the sustainable management of water resources (Ali & Aftab, 2022).

Effective watershed management is crucial to ensure the sustainability of our natural resources. It comprises of the socio-economic, biophysical, and human interrelationship among water, soil, land use, and ecosystem. The concept of watershed management involves taking into account socio-economic and institutional factors both within and outside the watershed area, while striving to minimize harm to natural resources (Aher et al., 2014; Ffolliott et al., 2012).Research reveals that if the watersheds are not managed in an integrated sustainable way, led to a diminution of natural resources i.e., water, vegetation, soil fertility, flora and fauna, etc(Ma, 2004).Understanding the scenario of GW resources is crucial for ensuring sustainable development in a region (Selvam et al., 2014).The GW recharge potential mapping and delineation is among the most important and prior stages in GW resources management and planning (Chen et al., 2018).

The utilization of geospatial technologies is essential for the successful exploration of groundwater and the effective management of watersheds. These innovative technologies enable the measurement, analysis, and visualization of geospatial data, thus facilitating the identification of water resources and the monitoring of hydrological processes. As such, geospatial technologies play a crucial role in the evaluation and management of water resources, aiding decision-makers in making informed and effective decisions that ensure sustainable water use. Geospatial technologies are a more efficient and cost-effective alternative to traditional methods. They allow for quicker completion of tasks, while also reducing overall costs (Faust et al., 1991; Gebrie et al., 2018; Israil et al., 2006).GIS coupled with MCDA covers a large area in a short period to map and identify GW recharge potential zones (Senthilkumar et al., 2019).Several researchers around the globe (Alam et al., 2022; Allafta et al., 2021; Argaz et al., 2019; Chandramohan et al., 2019; Dabral et al., 2014; Hayat et al., 2021; Kabeto et al., 2022; Maqsoom et al., 2022; Razandi et al., 2015; Sardar et al., 2022; Senthilkumar et al., 2019; Uc Castillo et al., 2022; V.Keshavan et al., 2017; Xu et al., 2021) have applied GIS and RS-based techniques for identification of GW recharge potential zones. They used GIS-based models like the Analytical hierarchy process (AHP), fuzzy logic, frequency ratio (FR), Multi-criteria decision analysis, Shannon's entropy, artificial neural network (ANT), etc.

A truly little geospatial technology-based approach has been adopted in the country as well as in the study area. This study employs geospatial technology to develop thevdelineation of GW recharge potential zones in the Quetta region of Pakistan. The research will apply remote sensing (RS) and geographic information system (GIS) along with the analytical hierarchy process (AHP), fuzzy-AHP, and frequency-ratio (FR) models. Mapping groundwater recharge potential zones will assist decision-makers in groundwater resource management and future land use planning.. In drought-prone regions where the GW table is relatively deep, ensuring a consistent supply of clean water has been a significant challenge. This study will also help in the installation of future dug/tube wells or boreholes in the study area which can minimize the cost and effort of hydrogeological investigation.

Methodology

Study area

Baluchistan is the largest province of Pakistan that spreads over an area of about 347,000 km². Geographically, it constitutes about 43% of the total area of the country. Hydrologically, Baluchistan is divided into 18 river basins, namely, Dasht, Gaj, Gawadar, Hab, Hamun-e-Lora, Hingol, Hmun-e-Mashkhel, Kachiplain, Kadnai, Kaha, Kand, Kundar, Mula, Nari, Pishin, Porali, Rakhshan, and Zhob. The Study area of Quetta region is a part of the Pishin River Basin, lies at Latitude from 29º45`00``to 30º30`00``, Longitude from 66º45`00 to 67º20'00 (shown in Fig, 1.).
The topography of the study area is varied and includes elongated mountain ridges, depressions, and small plains. The height of the sub-basin gradually rises as you move towards the northeast of Quetta Valley. This is where the Zarghoon Range is located, forming the highest peak in the area at 3,519 meters above sea level (masl). In Zargoon, the streams flow through gorges with extremely steep slopes. The Takatu Range of 3,401 masl is exposed in the north of the valley. The Chiltan Range is 3,261 masl exposed in the west and the Murder Ghar is 3,134 masl exposed to the east of the study area. The central part is somehow flat and gently sloping toward the south along the drainage pattern. The average topographic elevation of the study area is 1,650 masl.

.

Fig(1): Location map of Balochistan showing 18 River Basins. The enlarged map of Pishin River basin (orange color) shows nine subbasins including Quetta Subbasin (Study area) and the location of meteorological station Quetta(Ali & Aftab, 2022)

Datasets acquisition sources and preparation of thematic layers/maps

The acquisition of data is the most critical step in research. The selection of influencing factors is a key stage in GW recharge studies (A. A. Ahmed & Shabana, 2020; R. Ahmed & Sajjad, 2018).In the current study influencing factors were considered based on its importance to the GW recharge and extensive literature review. Thematic maps were constructed from satellite and conventional data by using ArcMap 10.8. A Digital Elevation Model (DEM) with a 30m resolution was downloaded from the open topography website (https://portal.opentopography.org/) and was further employed to generate thematic maps, such as slope, elevation, TWI, drainage density, and lineament density.

Geology thematic layer

Geology signifies the physical makeup of rocks including their mineral compositions and grain size arrangement, etc. (Freeze, 1984).The type of rock has a significant impact on how groundwater moves because it determines the flow mechanisms and infiltration (Jerbi et al., 2018; Tolche, 2021).In the current study geological map (1:250000 scale) was collected from a geological survey of Pakistan, and was rectified and digitized by using ArcGIS-10.8. Ultimately, the thematic map was transformed from vector to raster format prior to assigning weights and ranks (Fig, 2.A).

Lineament Density (LD) thematic layer

Lineaments provided valuable details on the underground geology and physical characteristics like fractures, faults, and joints. Lineaments express local and regional tectonic behavior; and also act as reservoirs and channels for hydrocarbons and mineral deposits (El-Sawy et al., 2016).The automatic line extraction in PC1 was done with Geomatica 2016. Discontinuities were verified using the "Split Line Tool" in ArcMaphe "Split Line Tool" in ArcMap. Ultimately, the density map of lineaments was created by employing the "Line Density Tool" in ArcMap (Fig, 2. B).

Soil types thematic layer

The infiltration process is greatly influenced by the texture of the soil, which makes soil one of the main influencing factors in GW recharge studies (Das, 2019).The soil map was downloaded from ISRIC (https://www.isric.org/). The study area comprised seven types of soil namely; calcisols, combisols, fluvisols, gypsisols, leptosols, luvisols, and regosols (Fig, 2. C).

Slope thematic layer

The slope represents the angle between the tangent plane and the horizontal plane at any given point (Maidment, 1993). The slope plays a crucial role in determining the flow formation process and infiltration rate (Simmers, 1990). Many of researchers reported an inverse relation between slope and infiltration rate (Chaplot & Le Bissonnais, 2000; Essig et al., 2009; Yuan et al., 2001). Gentle slope areas have a high infiltration rate, so more suitable for GW recharge and vice versa (Liu et al., 2018).The slope map of the study area was generated from DEM using the "Spatial Analysis tools" in ArcGIS 10.8.(Fig, 2.D). The study area includes steep areas, with high slopes found in the northern and eastern sections due to the mountainous terrain, making slope a key factor in the current study.

Topographic Wetness Index (TWI) thematic layer

TWI describes how topography affects hydrologic processes. It relates to GW flow movement and its retentions in subsurface zones(Raduła et al., 2018). TWI is computed as (Equation.1);

$$\mathrm{TWI} = \ln(\alpha | \tan \beta) \quad (1)$$

Where, α denotes Specific contributing area and β denotes Topographic slope of the area.

Areas with higher topographic wetness index (TWI) values are more suitable for GW recharge, as they indicate higher GW potential zones. This is in contrast to areas with lower TWI values. (Arulbalaji et al., 2019).To achieve this, in ArcMap, we first projected the digital elevation model (DEM) to WGS84/UTM Zone 42 N. Then, we followed a series of steps including filling the DEM, determining the flow direction and accumulation, calculating the slope in degrees, calculating the radiance of slope, and scaling the flow accumulation. Finally, we determined the TWI using the natural logarithm of the scaled flow accumulation divided by the tangent of the slope (Fig, 2.E).

Drainage Density (DD) thematic layer

Drainage density represents spatial distribution of the streams length per unit area (Adiat et al., 2012; Carlston, 2018; Selvam et al., 2016).Drainage density is one of the key factors in assessing and distribution of GW potentials over an area (Arshad et al., 2020b; Harinarayana et al., 2000; Saranya & Saravanan, 2020). It describe the occurrence and flow pattern of water under the surface(A. Khan et al., 2020; Selvam et al., 2016). The DD has an inverse relationship with the permeability (Chowdhury et al., 2010). DD and surface runoff have a direct relationship with each other. In regions with low DD, infiltration is greater compared to regions with high DD (Magesh et al., 2012) and good sources of high GW recharge (Srivastava & Bhattacharya, 2006).

The DD value is computed as (Equation.2) (Yeh et al., 2009):

$$\mathrm{DD} = \frac{\sum_{i=1}^{i=n} Si}{A} \quad (2)$$

Where, Si denotes the total length of drainage in km and A is the area in km².

The Stream Network was generated using "Hydrology Tool" in ArcMap. The following steps were taken: Fill DEM> Flow Direction> Flow Accumulation> Stream Order> Stream to Feature> and line density (Fig. 2.F).

Elevation thematic layer

Altitude is a crucial factor in GW recharge as it triggers water flow under gravity(R. Ahmed & Sajjad, 2018; Gebreyohannes et al., 2017). Studies have indicated that the transfer of water from higher to lower altitudes is more pronounced in mountainous regions due to their elevated levels. Moreover, it has been established that flat surfaces are more effective in recharging water sources as compared to inclined surfaces and high-altitude regions(Liu et al., 2018). The study area consists mostly of mountainous regions with steep altitudes, leading altitude to be a critical factor that impacts groundwater recharge in the study. (Fig. 2.G).

Land use land cover (LULC) thematic layer

The Land Use and Land Cover (LULC) is a crucial factor in determining appropriate locations for GW recharge (Singh et al., 2013). For the purposes of our current study, we utilized a LULC map that was conveniently available for download from the Living Atlas by Esri. The exact website that we obtained the map from can be found at https://livingatlas.arcgis.com/.The study area having six classes; waterbody, trees, cropland, builtup, barenland and rangeland (Fig, 2.H).

Rainfall thematic layer

The characteristics of rainfall affect infiltration, runoff, and GW recharge(Kotchoni et al., 2018; Mahalingam & Vinay, 2015). The study has obtained rainfall data from the department of irrigation, Balochistan. The data covers the last 30 years (1980 to 2010), and the average rainfall data from multi-rain gauge stations were interpolated using the “Spatial Analyst Tools” > Interpolation > IDW. This process produced a rainfall contour map that was used to extract the rainfall map for the study area by applying the "Spatial Analyst Tool" > Extraction > Extract by Mask (Fig, 2.I)

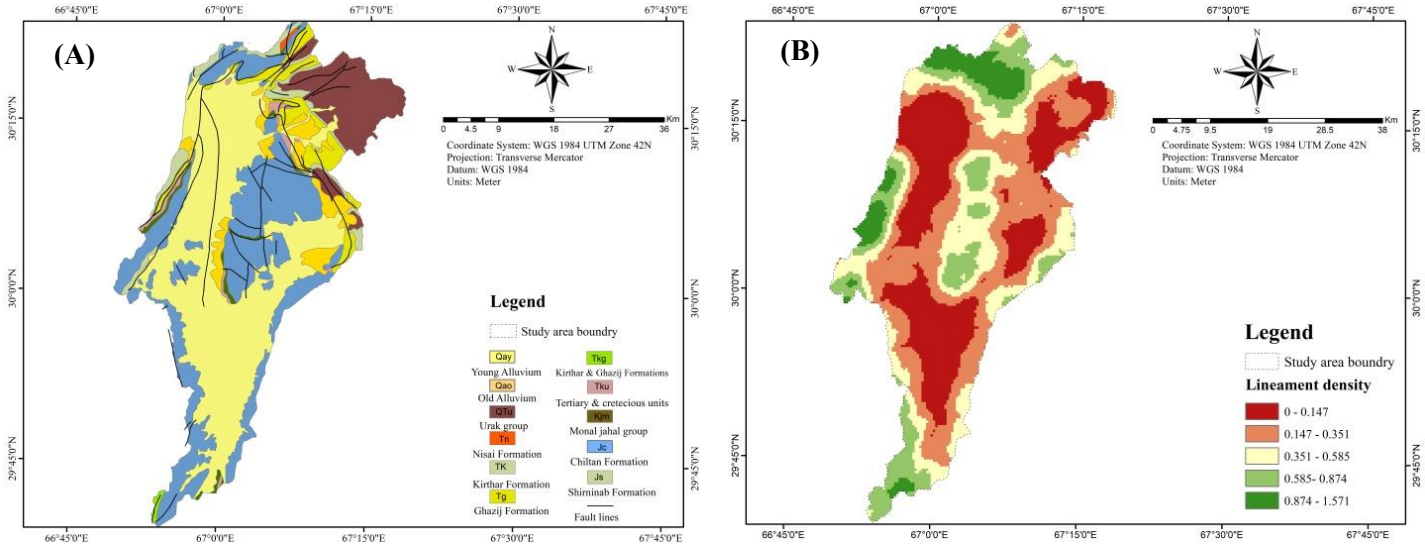

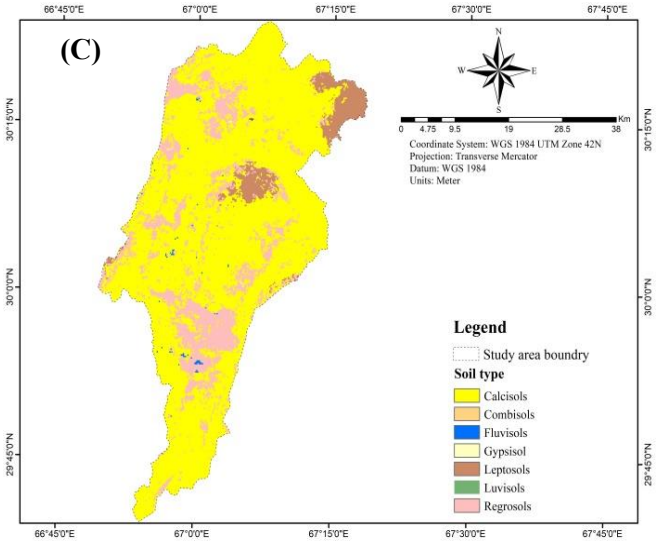
(C)
Coordinate System: WGS 1984 UTM Zone 42N
Projection: Transverse Mercator
Datum: WGS 1984
Units: Meter
Legend
Study area boundry
Soil type
Calcisols
Combisols
Fluvisols
Gypsisol
Leptosols
Luvisols
Regrosols

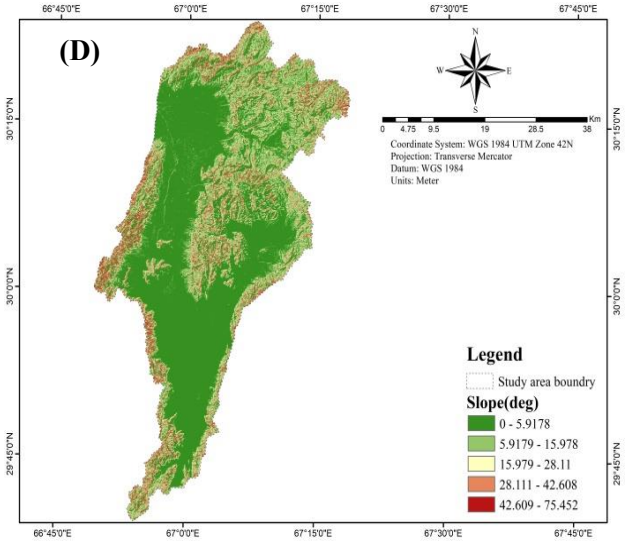
(D)
Coordinate System: WGS 1984 UTM Zone 42N
Projection: Transverse Mercator
Datum: WGS 1984
Units: Meter
Legend
Study area boundry
Slope(deg)
0 - 5.9178
5.9179 - 15.978
15.979 - 28.11
28.111 - 42.608
42.609 - 75.452

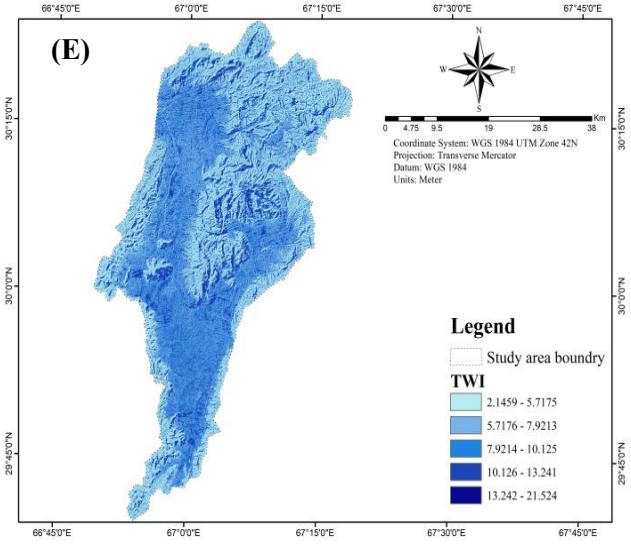
(E)
Coordinate System: WGS 1984 UTM Zone 42N
Projection: Transverse Mercator
Datum: WGS 1984
Units: Meter
Legend
Study area boundry
TWI
2.1459 - 5.7175
5.7176 - 7.9213
7.9214 - 10.125
10.126 - 13.241
13.242 - 21.524

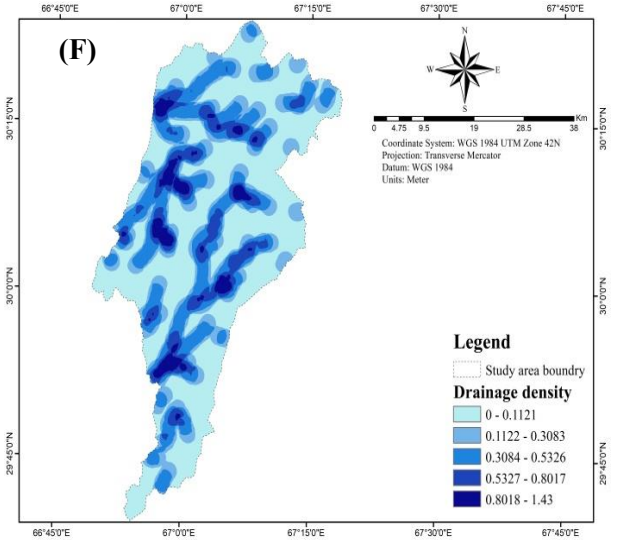
(F)
Coordinate System: WGS 1984 UTM Zone 42N
Projection: Transverse Mercator
Datum: WGS 1984
Units: Meter
Legend
Study area boundry
Drainage density
0 - 0.1121
0.1122 - 0.3083
0.3084 - 0.5326
0.5327 - 0.8017
0.8018 - 1.43

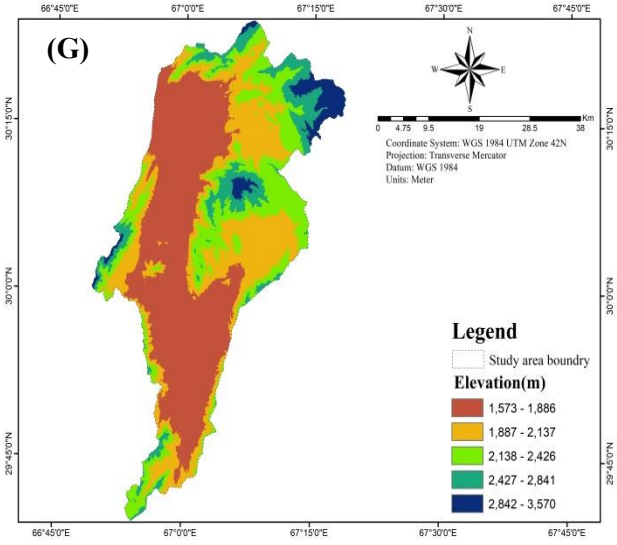
(G)
Coordinate System: WGS 1984 UTM Zone 42N
Projection: Transverse Mercator
Datum: WGS 1984
Units: Meter
Legend
Study area boundry
Elevation(m)
1,573 - 1,886
1,887 - 2,137
2,138 - 2,426
2,427 - 2,841
2,842 - 3,570

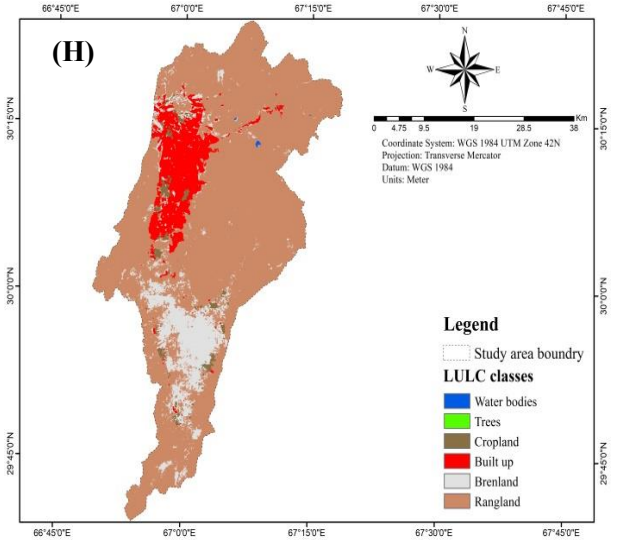
(H)
Coordinate System: WGS 1984 UTM Zone 42N
Projection: Transverse Mercator
Datum: WGS 1984
Units: Meter
Legend
Study area boundry
LULC classes
Water bodies
Trees
Cropland
Built up
Brenland
Rangland

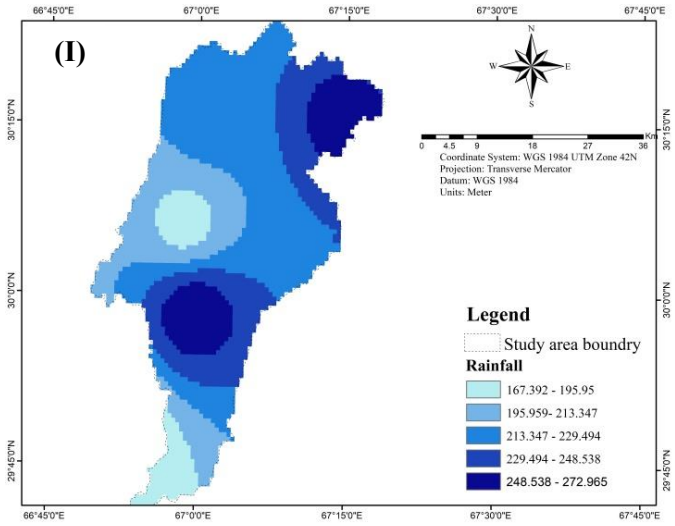

Fig(2): Thematic/factors maps (A)Geology(B)Lineament density (C) Soil type (D) Slope (E)TWI (F) drainage density(G)Elevation (H)LULC (I)Rainfall.

Methodological overview

The current study utilizes a multi-parameter dataset consisting of geology, lineament density, drainage density, soil type, slope, elevation, TWI, average rainfall, and LULC to identify GW recharge potential zones. The study employs three models -AHP, FAHP, and FR - to delineate these zones, providing a comprehensive understanding of the factors that contribute to GW recharge potential in the area. The methodological framework for this study is outlined in Figure 3. The mapping of the GW recharge zone is divided into four stages, as given below.

Stage 1.Data acquisition and database generation: In the initial stage, a thorough evaluation was conducted to identify nine key factors that impact GW recharge zones. Based on this evaluation, a comprehensive geospatial database was created, which forms the foundation for further analysis.

Stage.2 Preprocessing and the generation of thematic maps: The second stage included preprocessing of all acquired data and generating thematic maps from satellite and conventional data using the ArcGIS environment.

Stage.3 Weight assignment and reclassification of thematic layers: In the third stage of analysis, three models were employed to assign weights to different thematic maps based on their importance to GW recharge. These maps were then divided into three distinct classes, which corresponded to high, moderate, and low recharge zones. To produce final maps of GW recharge potential, various techniques such as AHP-Weighted linear combination, AHP-Weighted sum, fuzzy-AHP overlay, and FR-based models were used in ArcGIS. By merging all the layers, the final maps were created.

Stage.4 Results validation: In the fourth and final stage, the results were validated to ensure their accuracy. This was done through the use of receiver operating characteristics (ROC) curves for each of the models (AHP, FAHP, and FR). Additionally, the electrical conductivity of wells was used for cross-validation. The final results have been verified using these methods.

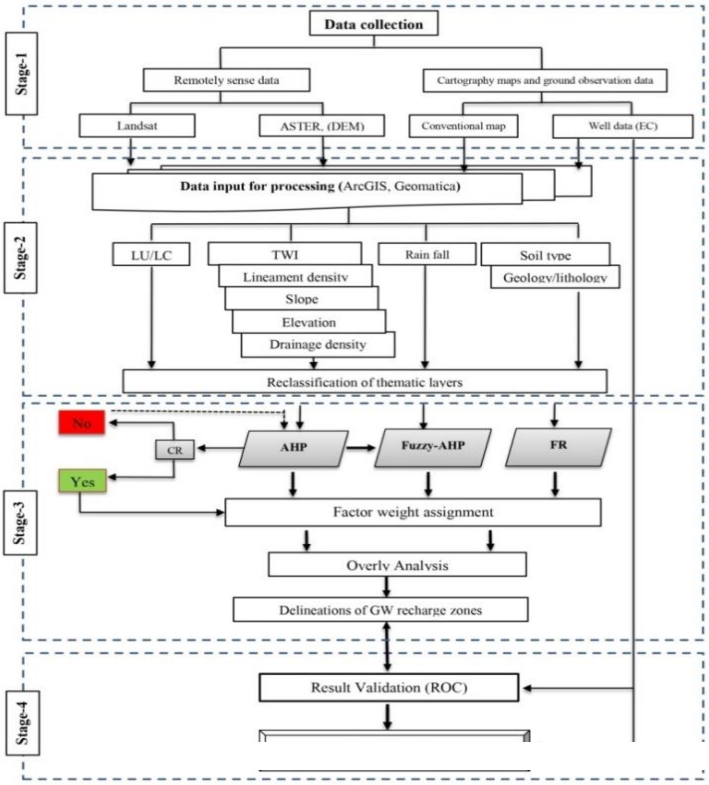

Fig(3): Methodological flowchart of the current study

Results and Discussions

AHP model-based weight assignment

Thomas Saaty developed the Analytic Hierarchy Process (AHP) at the Wharton School of Business in 1980. It offers decision-makers a method to analyze and address intricate issues within a hierarchical framework. It clearly displays the relationships among goals, objectives, sub-objectives, and alternatives (Dabral et al., 2014). The AHP method was used in ArcGIS to determine the Normalized Principal Eigenvector (NPEV) or Percent Weight in the weighted overlay Analysis. The process involves entering contributing criteria based on their importance in mapping GW recharge zones. Factors are given scores between 1-9,indicating their relative importance in pairwise comparisons(Saaty, 1980).A pairwise comparison matrix (PCM) was constructed based on saaty scale and expert opinion (shown in table.1).

Table (1): Analytic hierarchy process pairwise compression matrix (PCM)

PCM	GE	ST	SL	LULC	LD	EL	TWI	DD	RF
GE	1	1	2	3	3	3	5	5	5
ST	1	1	1	2	3	3	5	5	5
SL	0.50	1	1	2	3	3	4	5	5
LULC	0.33	0.50	0.50	1	2	3	5	5	4
LD	0.33	0.33	0.33	0.50	1	1	3	4	2
EL	0.33	0.33	0.33	0.33	1	1	3	3	3
TWI	0.20	0.20	0.25	0.20	0.33	0.33	1	1	1
DD	0.20	0.20	0.20	0.20	0.25	0.33	1	1	1
RF	0.20	0.20	0.20	0.25	0.50	0.33	1	1	1
Σ(columns)	4.10	4.77	5.82	9.48	14.08	15.00	28.00	30.00	27.00

Where, GE represents geology, ST represents soil type, SL represents slope, LULC represents land use/land cover, LD denotes lineament density, EL denotes elevation, DD denotes drainage density, TWI represents topographic wetness index and RF represents rainfall.

Once the Pairwise comparison matrix was created, normalized weights (Wn) were computed

Table (2): Normalized relative weight (Wn) and Normalized Principal Eigen Vector (NPEV).

NPCM	GE	ST	SL	LULC	LD	EL	TWI	DD	RF	Eigen Vector	NPEV (%)
GE	0.244	0.210	0.344	0.316	0.213	0.200	0.179	0.167	0.185	0.229	22.9
ST	0.244	0.210	0.172	0.211	0.213	0.200	0.179	0.167	0.185	0.198	19.8
SL	0.122	0.210	0.172	0.211	0.213	0.200	0.143	0.167	0.185	0.180	18.0
LULC	0.081	0.105	0.086	0.105	0.142	0.200	0.179	0.167	0.148	0.135	13.5
LD	0.081	0.070	0.057	0.053	0.071	0.067	0.107	0.133	0.074	0.079	7.9
EL	0.081	0.070	0.057	0.035	0.071	0.067	0.107	0.100	0.111	0.078	7.8
TWI	0.049	0.042	0.043	0.021	0.024	0.022	0.036	0.033	0.037	0.034	3.4
DD	0.049	0.042	0.034	0.021	0.018	0.022	0.036	0.033	0.037	0.032	3.2
RF	0.049	0.042	0.034	0.026	0.036	0.022	0.036	0.033	0.037	0.035	3.5
Σ(columns)	1	1	1	1	1	1	1	1	1		100.0

Finally Normalized weights (wn) were verified using consistency ratio matrix (Saaty, 1980).

A Consistency Ratio (CR) is the ratio of the Consistency Index (CI) to the Random Consistency Index. (RI).The value of CI for GW potential and recharge zone parameters investigated in this study was calculated as (Equation.3);

$$CI = \frac{\lambda max - n}{n - 1} \quad (3)$$

Where n represents the quantity of criteria (thematic layers in this study) and λmax stands for the Principal Eigenvalue value(Ratio of weight sum to the criteria weight) obtained from consistency ratio matrix (Table.4). The Random index (RI) was derived from Table 3.of Satty (1980), which depends on number of criteria (n) adopted in study

Table 3:Random Index (RI) value related to the number of criteria (n).(Saaty, 1980)

n	1	2	3	4	5	6	7	8	9	10
RI	0	0	0.58	0.9	1.12	1.24	1.32	1.41	1.45	1.49

The CR value is utilized to evaluate the consistency of the matrix.The CR value must be determined less than 0.1(Malczewski, 1999; Saaty, 1980).If the value of CR is less than or equal to 0.1(10%), the inconsistency is acceptable. However, if the CR value is higher than 0.1(10%), then the comparison judgment must be re-evaluated. In the present study the λmax value obtained is 9.274 and RI is 1.45 (from table 3).The value of CR=0.023 < 0.10, which suggest that the inconsistency is acceptable for this 9 parameters under consideration in current study.

Table (4): Consistency Ratio Matrix

Matrix	GE	ST	SL	LULC	LD	EL	TWI	DD	RF	ΣWeight	λmax
GE	0.229	0.198	0.361	0.404	0.238	0.233	0.170	0.162	0.175	2.170	9.494
ST	0.229	0.198	0.180	0.270	0.238	0.233	0.170	0.162	0.175	1.855	9.380
SL	0.114	0.198	0.180	0.270	0.238	0.233	0.136	0.162	0.175	1.707	9.469
LULC	0.076	0.099	0.090	0.135	0.159	0.233	0.170	0.162	0.140	1.265	9.383
LD	0.076	0.066	0.060	0.067	0.079	0.078	0.102	0.130	0.070	0.729	9.194
EL	0.076	0.066	0.060	0.045	0.079	0.078	0.102	0.097	0.105	0.709	9.120
TWI	0.046	0.040	0.045	0.027	0.026	0.026	0.034	0.032	0.035	0.311	9.130
DD	0.046	0.040	0.036	0.027	0.020	0.026	0.034	0.032	0.035	0.296	9.103
RF	0.046	0.040	0.036	0.034	0.040	0.026	0.034	0.032	0.035	0.322	9.196

Before applying weighted overlay analysis, the ranks were assigned to each factor of all thematic layers, and the weight was assigned according to their relative importance to GW recharge potential using the Analytic Hierarchical Process (AHP) technique (Brunelli, 2014).After assigning weights to all thematic layers, ranks/scale values from 1 to 3 were given for the sub variable of every thematic layer, in line with their importance for GW recharge potential occurrence. According to this study, 1 represents less vital (low recharge zones), and 3 represents more vital (high recharge) for GW recharge potential zoning. Final weighted overlay was calculated (Fig, 5.A).

In weighted sum, all classified thematic were multiplied with their corresponding weights and sum in the " weighted sum" tool in overlay analysis (Fig, 5B).

Table (5): Thematic layer rank and weight in terms of GW recharge perspective

Thematic layer	Feature Classes	GWR Perspective	Rank assigned	Weight (%)
Geology	Tg/ KJm/ TKu/ Tk/ Tkg/ Tn/Js	Low	1	23
	QTu/Jc	Moderate	2	
	Qay/Qao	High	3	
Soil Type	Gypsisols/ Regosols	Low	1	20
	Luvisol/ Combisols	Moderate	2	
	Calcisols/ Fluvisols/ Leptosols	High	3	
Slope(degree)	29.88 - 75.45	Low	1	18
	10.35 - 29.88	Moderate	2	
	0-10.35	High	3	
LULC	Built Up/ Bare land/ Rangland	Low	1	13
	Waterbodies/ Trees/ CropLand	High	3	
Lineament Density	0 - 0.308	Low	1	8
	0.308 - 0.696	Moderate	2	
	0.696 - 1.571	High	3	
Elevation(m)	488.93 - 3569.53	Low	1	8
	1987.789 - 2488.9	Moderate	2	
	1572.776 - 1987.7	High	3	
TWI	2.145925 - 6.3848	Low	1	03
	6.384852 - 9.7154	Moderate	2	
	9.715438 - 21.523	High	3	
Drainage Density (km/km²)	0.560598 - 1.4295	Low	1	03
	0.196209 - 0.5605	Moderate	2	
	0 - 0.196209	High	3	
Rainfall(mm)	167.392 - 209.207	Low	1	04
	209.207 - 237.360	Moderate	2	
	237.360 - 272.965	High	3	

FAHP model-based weight assignment

The Fuzzy-Analytic Hierarchy Process (FAHP) is a decision-making model that combines the AHP method with fuzzy logic theory. This hybrid model is designed to handle uncertainty and vagueness in the decision-making process. In simpler terms, fuzzy logic theory is used to apply the theory of fuzzy sets in decision-making(Zadeh, 1965). The fuzzy set theory is a mathematical framework for dealing with uncertainty and vagueness in data by allowing partial membership in a set (Tiwari et al., 2017). Fuzzy set values range from 0 to 1, indicating gradual class transition(Mallick et al., 2019). Fuzzy-AHP was used to upgrade the AHP analysis by introducing fuzzy weight. The analysis involved two stages. In the first stage of the analysis, weight was assigned to each thematic layer based on pairwise-comparison matrices and triangular fuzzy numbers (TFNs). The TFNs are represented by *l* (lowest possible value), *m* (most likely possible value),and *u* (highest possible value) (shown in Table 6.a-b).In the second step the geometric mean and the fuzzy weights for the thematic layers were calculated by employing Buckley's geometric mean method
(Equations. 4 and 5).(Buckley, 1985)

$$Ri = (a_{i1} \otimes a_{i2} \otimes \ldots\ldots \otimes a_{in})^{1/n} \quad (4)$$

$$Wi = R_i \otimes (R_1 \oplus R_2 \oplus \ldots\ldots R_n)^{-1} \quad (5)$$

Where *Ri* denotes the geometric mean values of criterion *i* to each criterion and a_{in} is fuzzy comparisons value of criterion *i* to criterion *n*; Wi is the fuzzy-weight of the i^{th} criterion(Mallick et al., 2019).

Table (6): a. Fuzzy pairwise comparison matrix (FPCM)

FPCM	GE	ST	SL	LULC	LD	EL	TWI	DD	RF
GE	(1,1,1)	(1,1,1)	(1,2,3)	(2,3,4)	(2,3,4)	(2,3,4)	(4,5,6)	(4,5,6)	(4,5,6)
ST	(1,1,1)	(1,1,1)	(1,1,1)	(1,2,3)	(2,3,4)	(2,3,4)	(4,5,6)	(4,5,6)	(4,5,6)
SL	(0.33,0.50,1.00)	(1,1,1)	(1,1,1)	(1,2,3)	(2,3,4)	(2,3,4)	(3,4,5)	(4,5,6)	(4,5,6)
LULC	(0.25,0.33,0.50)	(0.33,0.50,1.00)	(0.33,0.50,1.00)	(1,1,1)	(1,2,3)	(2,3,4)	(4,5,6)	(4,5,6)	(3,4,5)
LD	(0.25,0.33,0.50)	(0.25,0.33,0.50)	(0.25,0.33,0.50)	(0.33,0.50,1.00)	(1,1,1)	(1,1,1)	(2,3,4)	(3,4,5)	(1,2,3)
EL	(0.25,0.33,0.50)	(0.25,0.33,0.50)	(0.25,0.33,0.50)	(0.25,0.33,0.50)	(1,1,1)	(1,1,1)	(2,3,4)	(2,3,4)	(2,3,4)
TWI	(0.17,0.20,0.25)	(0.17,0.20,0.25)	(0.20,0.25,0.33)	(0.17,0.20,0.25)	(0.25,0.33,0.50)	(0.25,0.33,0.50)	(1,1,1)	(1,1,1)	(1,1,1)
DD	(0.17,0.20,0.25)	(0.17,0.20,0.25)	(0.17,0.20,0.25)	(0.17,0.20,0.25)	(0.20,0.25,0.33)	(0.25,0.33,0.50)	(1,1,1)	(1,1,1)	(1,1,1)
RF	(0.17,0.20,0.25)	(0.17,0.20,0.25)	(0.17,0.20,0.25)	(0.20,0.25,0.33)	(0.33,0.50,1.00)	(0.25,0.33,0.50)	(1,1,1)	(1,1,1)	(1,1,1)

The Fuzzy weights were later standardized in order to determine the weight of each criteria (6.b) utilizing (Equation.6);

$$Ni = \frac{Mi}{\sum_{i=1}^{n} Mi} \quad (6)$$

Where Mi=*lwi*+*mwi*+*uwi*/3, and Ni=1, i=*1,2….n. lwi* , *mwi* , *uwi* represents the lower, middle, and upper values of the fuzzy weights of the *ith* criterion, respectively.

Table (6):b. Fuzzy geometric mean (Ri), fuzzy-weight (Wi), and normalized weight (Ni) of each criterion

	Fuzzy geometric mean (*Ri*)			*Mi*			Fuzzy Weight (*Wi*)	Normalized weight (*Ni*)
				l	*m*	*u*		
GE	2.00	2.66	3.26	0.134	0.228	0.365	0.2428	0.217
ST	1.85	2.36	2.79	0.124	0.202	0.312	0.2133	0.191
SL	1.59	2.13	2.74	0.107	0.182	0.306	0.1988	0.178
LULC	1.12	1.54	2.17	0.075	0.132	0.243	0.1504	0.135
LD	0.68	0.91	1.25	0.045	0.078	0.140	0.0881	0.079
EL	0.68	0.89	1.17	0.045	0.075	0.130	0.0842	0.075
TWI	0.34	0.39	0.48	0.022	0.033	0.053	0.0367	0.033
DD	0.32	0.37	0.44	0.112	0.031	0.049	0.0648	0.058
RF	0.35	0.41	0.52	0.023	0.035	0.057	0.0389	0.035

In the second phase of the analysis, fuzzy membership values were allocated to the each thematic layer. The ArcGIS platform was utilized to assign the fuzzy membership values by employing the linear transformation function. The fuzzy linear transformation is a frequently utilized technique in research related to GW recharge(Aouragh et al., 2017). After the linear transformation of classified maps, normalized fuzzy weights were multiplied with each thematic map using a raster calculator in the spatial analyst tool. Finally, fuzzy overlay analysis was employed to get the final GW recharge zones map. The Final map was reclassified into three GW recharge potential zones viz. high, moderate, and low recharge zones (Fig, 5. C)

FR model-based weight assignment

The FR model is a statistical model that can be used to assess the relationship between independent and dependent variables in geospatial analysis. This model is bi-variate and provides a convenient way to define the probability of this relationship. Additionally, the FR model can be applied to multi-classified maps, making it a versatile tool for geospatial analysis(Oh et al., 2011). Many researchers have successfully applied FR models for GW recharge mapping (Arshad et al., 2020a; Manap et al., 2014; Moghaddam et al., 2015; Ozdemir, 2011; Pourtaghi & Pourghasemi, 2014a). The

structural composition of the FR model relies heavily on the correlations and observed relationships between each groundwater conditioning factor and the distribution of well locations. The FR value attributed to each class of groundwater-related factors can be effectively expressed via the utilization of Equation.7;

$$FR = \frac{\frac{W}{G}}{\frac{M}{T}} \quad (7)$$

Where W denotes the count of pixels with GW wells and G represent the total number of GW wells within the study area. M represents the number of pixels within the class area of the factor, while T represents the total count of pixels within the study area. In a given pixel, GW potential can be determined by the summation of pixel values according to the Equation. 8;

$$GRPZ = \sum_{i=1}^{n} FRi \quad (8)$$

Where Where GRPZ represents the GW recharge potentials zones and FRi is the FR value of each factor.
In comparison to AHP and FAHP, in FR technique, the weight to the each class is not assigned on the bases of properties of the influencing factors but given on the bases of spatial occurrence of the wells in each class. Similarly, the FR is calculated for all the conditioning factors (Table.7). Finally, the GW recharge zones map has been created by using raster calculator in ArcGIS environment (Fig, 5.D)

Table (7): Frequency ratio values for each thematic layer and its classes.

Thematic layers	Assigned rank	Number of pixels in domain	Percentage of domain	Number of wells	Percent of wells	FR
GE	1	248378	11.98	5	6.67	0.56
	2	821228	39.61	4	5.33	0.45
	3	1003759	48.41	66	88.00	7.35
LD	1	1119729	53.96	63	84.00	1.56
	2	682608	32.90	11	14.67	0.27
	3	272740	13.14	1	1.33	0.02
DD	1	256820	12.39	15	20.00	1.61
	2	675677	32.59	22	29.33	2.37
	3	1140980	55.03	38	50.67	4.09
RF	1	615263	29.68	28	37.33	1.26
	2	941832	45.43	47	62.67	2.11
	3	516018	24.89	0	00.00	0.00
ST	1	369915	17.84	11	14.67	0.82
	2	7726	0.37	0	0.00	0.00
	3	1696393	81.79	64	85.33	1.04
SL	1	209427	10.18	4	5.33	0.52
	2	425130	20.67	1	1.33	0.13
	3	1422180	69.15	70	93.33	9.17
TWI	1	736991	35.83	12	16.00	0.45
	2	802555	39.02	9	12.00	0.31
	3	517191	25.15	54	72.00	2.86
EL	1	219230	10.57	1	1.33	0.13
	2	795597	38.37	1	1.33	0.13
	3	1058650	51.06	73	97.33	9.21
LULC	1	2040414	98.42	75	100.00	1.02
	3	32831	1.58	0	0.00	0.00

Thematic layers reclassification according to GW rechargeability

Geology & Reclassified Geology Layer

Lithology refers to the physical characteristics of rocks, including mineral composition and grain size (Freeze, 1984). Lithology controls the infiltration and flow processes of GW (Jerbi et al., 2018; Tolche, 2021). The study area is mostly covered by young alluvium (Qay), which makes up 46% of the area, followed by chiltan formation (Jc) at 29.8%, Urak formation (QTu) at 8%, old alluvium (Qao) at 5.2%, Ghazij formation (Tg) at 4.5%, Shirinab formation (Js) at 2.4%, kirthar formation (Tk) at 1.4%, Tertiary and cretaceous (Tku) at 1.3%, Monal jahal formation (Kjm) at 1% and Nasai formation (Tn) at 0.2%. The major lithologies exposed in wide areas are limestone, conglomerates, and sandstone. Geology was reclassified into three recharge potential classes based on permeability and porosity: low (Tg/KJm/TKu/Tk/Tkg/Tn/Js), moderate (QTu/Jc), and high (Qay/Qao) (Fig, 4a).

Lineament density & Reclassified Lineament density Layer

Lineaments are critical geological features that act as reservoirs and conduits for minerals and hydrocarbons and reveal local and regional tectonic behavior (El-Sawy et al., 2016). The Chaman Fault's tectonic movements have caused the formation of various folding, faulting, fractures and joint systems in the limestone formations of the area. These fractured zones and joint systems show promise for the occurrence and movement of GW. The lineaments may lead to the development of secondary porosity and permeability in rocks(Freeze, 1984; Maidment, 1993). Therefore high lineament density areas are likely to have significant potentials for GW recharge. Lineament density map was reclassified using natural breaks (Jenks) into three classes; Low (0-0.308), moderate (0.308-0.696), and high (0.696 - 1.571) (Fig, 4b).

Soil types & Reclassified Soil types Layer

The area under study consists of seven distinct soil types: Calcisols, cambisols, fluvisols, gypsisols, leptosols, luvisols, and regosols. Calcisols are the most prevalent soil type, covering 1347.64km² of the study area. Regosols cover nearly 300km², while leptosols cover 88.36 km², cambisols cover 5.5 km², fluvisols cover 3 km², gypsisols cover 0.65km², and luvisols cover an area of 0.1 km². (https://soilgrids.org/).The classification of the soils was revised based on their grain size and the proportion of sand, clay, and silt in them. (https://www.isric.org/).Coarse-grained soils are known for their ability to infiltrate water at a high rate and are given high recharge potential values (Brady et al., 2008; FitzPatrick, 1978). The reclassified soil type map shows leptosols, fluvisol, and calcisol characterize the high recharge areas because they are coarse-grained and have high sand contents (De Wit & Nachtergaele, 1990). Moderate value is assigned to cambisols and luvisols due to their ability to hold water well and good internal drainage. (P.M. & R. Dudal, 1989).Regosols and gypsisol have mostly high clay and fine texture(P.M. & R. Dudal, 1989),therefore assigned low recharge potentiality(Fig, 4c).

Slope & Reclassified Slope Layer

Slope has an inverse relation between infiltration rate (Chaplot & Le Bissonnais, 2000; Essig et al., 2009; Yuan et al., 2001).The areas with gentle slopes have high infiltration rate, so more suitable to GW recharge and vice versa (Liu et al., 2018; Simmers, 1990).In the mountainous region high slope is the main impediment in GW recharge whereas low slopes are favorable for GW recharge. Accordingly slope map was reclassified using natural breaks (Jenks) into three classes; Low (2.145- 6.384), moderate (6.384- 9.715), and high (9.715 - 21.523) GW recharge zones (Fig, 4d).

TWI & Reclassified TWI Layer

TWI describes the impact of topography on hydrologic processes. It relates GW flow movement and its retentions in subsurface zones (Raduła et al., 2018).There is a positive correlation between TWI and GW recharge potentials. Higher TWI values shows a higher GW potential zones so areas with higher TWI are more suitable for GW recharge as compared to area with low TWI values (Arulbalaji et al., 2019; Nampak et al., 2014; Yıldırım, 2021).TWI map was reclassified using natural breaks (Jenks) into three classes; Low (2.145 - 6.384), moderate (6.384 - 9.715), and high (9.715 - 21.523) GW recharge zone (Fig, .4e).

Drainage density & Reclassified Drainage density Layer

The Drainage density is a crucial factor in the assessment and distribution of GW potentials in an area (Arshad et al., 2020b; Harinarayana et al., 2000; Saranya & Saravanan, 2020).In terms of GW recharge, low drainage density implies

more infiltration (Magesh et al., 2012) and good sources of high GW recharge potentials (Srivastava & Bhattacharya, 2006). Accordingly, Low drainage density areas were given more importance than high drainage density areas, as illustrated in Fig. 4f. The drainage density map has been reclassified using natural breaks (Jenks) into three classes marked as low (0.560 - 1.429), moderate (0.196 - 0.560) and high (0 - 0.196), recharge zones.

Elevation & Reclassified Elevation Layer

The study area comprised of mountainous regions having high elevations. Based on GW rechargeability, elevation has been reclassified using natural breaks (Jenks) into three classes Low (488.93 - 3569.53), moderate (1987.789 - 2488.9), and high (1572.776 - 1987.7). The recharge potential of flat surfaces is greater than that of inclined surfaces and higher elevations, resulting in a higher rank being assigned to lower elevations (Liu et al., 2018) (Fig, 4g).

LULC & Reclassified LULC Layer

The LULC is an important indicator that helps in identifying suitable locations for GW (GW) recharge(Singh et al., 2013).LULC comprised of areal distribution soil, vegetation cover, cropland and residential. The study area have six classes; waterbody, trees, cropland, builtup, barenland and rangeland (Fig,2(H)).According to GW recharge perspective the LULC has been classified into two classes (Fig, 4h).The vegetation cover, waterbody and cropland assigned high weight as it has high GW inflation (Shaban et al., 2006),while builtup, barenland and rangland assigned low weight because of having high run-off and low infiltration rate (Anbazhagan et al., 2005).

Rainfall & Reclassified Rainfall Layer

The study area falls in semiarid-arid region receiving average rainfall of 180-250mm/annul. The province is affected by two different meteorological systems (Western disturbances and Monsoon). In extreme cases oceanic currents and monsoon currents originating from the Arabian Sea can also reach southern part of the watershed and cause significant rainfall. In the north Western disturbances are the major cause of rainfall. Western disturbances are predominant in northern areas and high rainfalls occur. Monsoon is predominant more in southern parts.(*I & P Department,GOB.*, 2016).The generated rainfall map has been reclassified using natural breaks (Jenks) into three classes marked as low (167.392 - 209.207), moderate (209.207 - 237.360) and high (237.360 - 272.965), recharge potential zones (Fig, 4i).

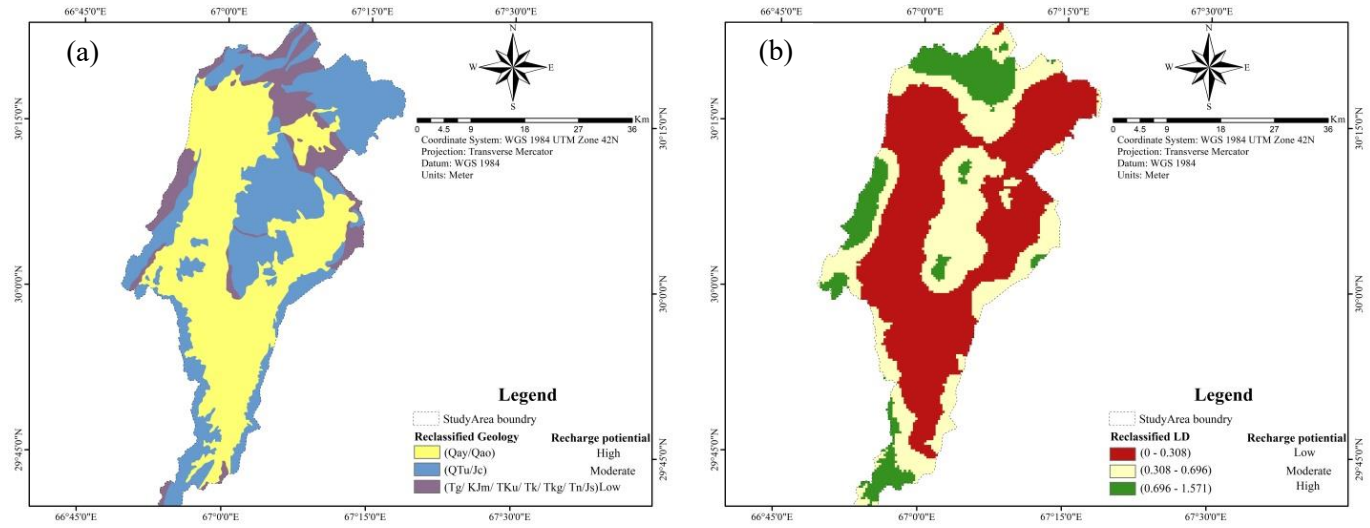

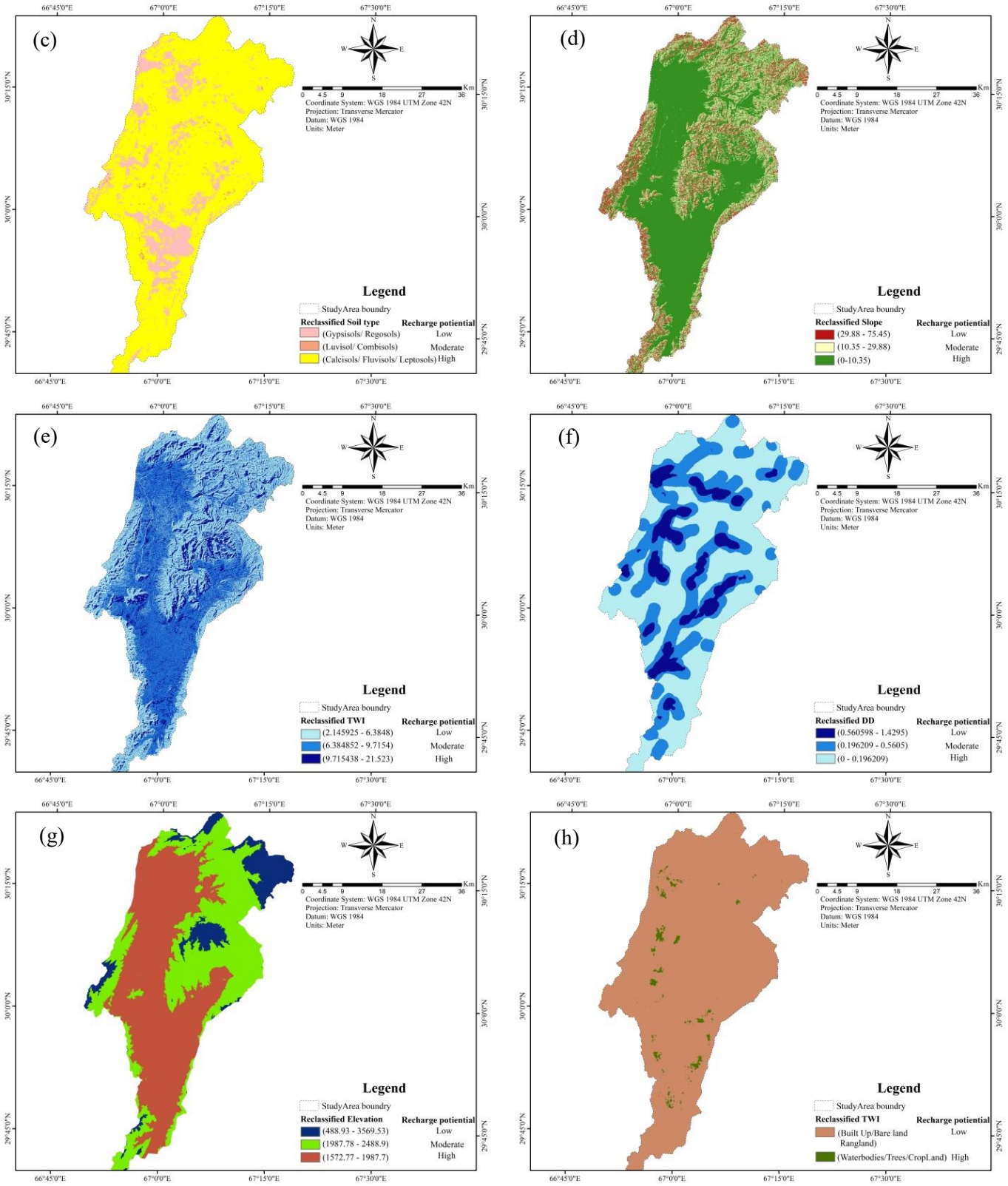
(c)
Coordinate System: WGS 1984 UTM Zone 42N
Projection: Transverse Mercator
Datum: WGS 1984
Units: Meter
Legend
StudyArea boundry
Reclassified Soil type
Recharge potential
(Gypsisols/ Regosols) Low
(Luvisol/ Combisols) Moderate
(Calcisols/ Fluvisols/ Leptosols) High
(d)
Reclassified Slope
(29.88 - 75.45) Low
(10.35 - 29.88) Moderate
(0-10.35) High
(e)
Reclassified TWI
(2.145925 - 6.3848) Low
(6.384852 - 9.7154) Moderate
(9.715438 - 21.523) High
(f)
Reclassified DD
(0.560598 - 1.4295) Low
(0.196209 - 0.5605) Moderate
(0 - 0.196209) High
(g)
Reclassified Elevation
(488.93 - 3569.53) Low
(1987.78 - 2488.9) Moderate
(1572.77 - 1987.7) High
(h)
Reclassified TWI
(Built Up/Bare land Rangland) Low
(Waterbodies/Trees/CropLand) High

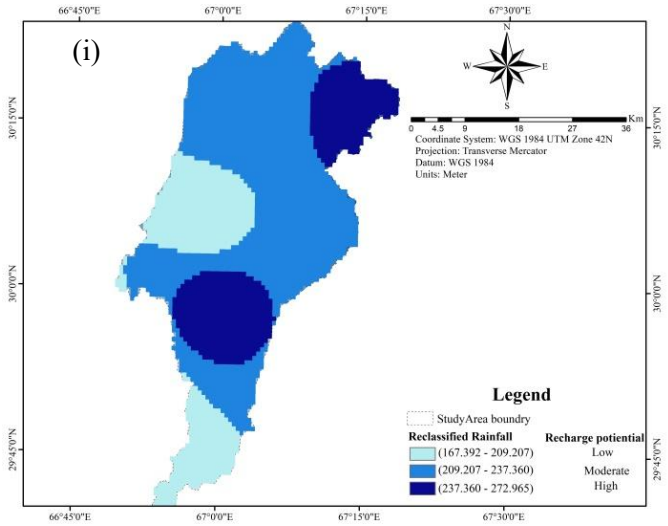

Fig(4): Reclassified Layers (a) Geology (b) Lineament density (c) Soil type (d) Slope (e) TWI(f) drainage density (g)Elevation (h)LULC (i) Rainfall.

Final GW recharge potential zones mapping in ArcGIS environment

Prior to the overlay analysis, all thematic layers underwent projection using WGS84/UTM Zone 14 N datum coordinate system. This was carried out to ensure a uniform resolution of 29*29m for optimal utilization within the ArcGIS environment.The GW recharge maps were created by overlaying all reclassified thematic layers (Geology, Soil type, Slope, LULC, Elevation, Lineament density, Drainage density, TWI, Rainfall) in the ArcGIS environment, as illustrated in Figure 4.a-i. To determine the final weight for each thematic layer, we used the AHP, FAHP, and FR models, which are outlined in Tables 5, 6.b, and 7. The resulting maps were then divided into three descriptive zones based on the recharge zone, namely "Low," "Moderate," and "High," each represented by distinct colors, as shown in Figures 5.A-D.

Table 8 displays the statistical and spatial distribution of each model (Fig. 5. A-D). The results of the AHP model-l show that 1449 km² (84%) of the study area falls under the moderate GW recharge zone, 254 km² (15%) falls under the high recharge zone, and 19 km² (1%) falls under the low recharge zone. On the other hand, the AHP model-ll indicates that 321 km² (19%) of the area falls under the low recharge zone, 721 km² (42%) falls under the moderate zone, and 680 km² (39%) falls under the high recharge zone. Similarly, the FAHP model reveals that 269 km² (16%) of the region falls under the low zone, 718 km² (42%) falls under the moderate zone, and 736 km² (43%) falls under the high recharge zone. Finally, the FR model statistics show that 391 km² (23%) of the area falls under the low zone, 610 km² (35%) falls under the moderate zone, and 721 km² (42%) of the study area falls under the high recharge zone.

Table (8): Spatial distribution of GW recharge zone

GWR zones	AHP Model-l		AHP Model-ll		FAHP Model		FR Model	
	Area (Km²)	Area (%)	Area (Km²)	Area (%)	Area (Km²)	Area (%)	Area(Km²)	Area (%)
Low	18.53	1.08	321.09	18.64	268.54	15.59	391.04	22.71
Moderate	1449.28	84.15	721.31	41.88	717.93	41.69	609.73	35.40
High	254.40	14.77	679.81	39.47	735.75	42.72	721.45	41.89

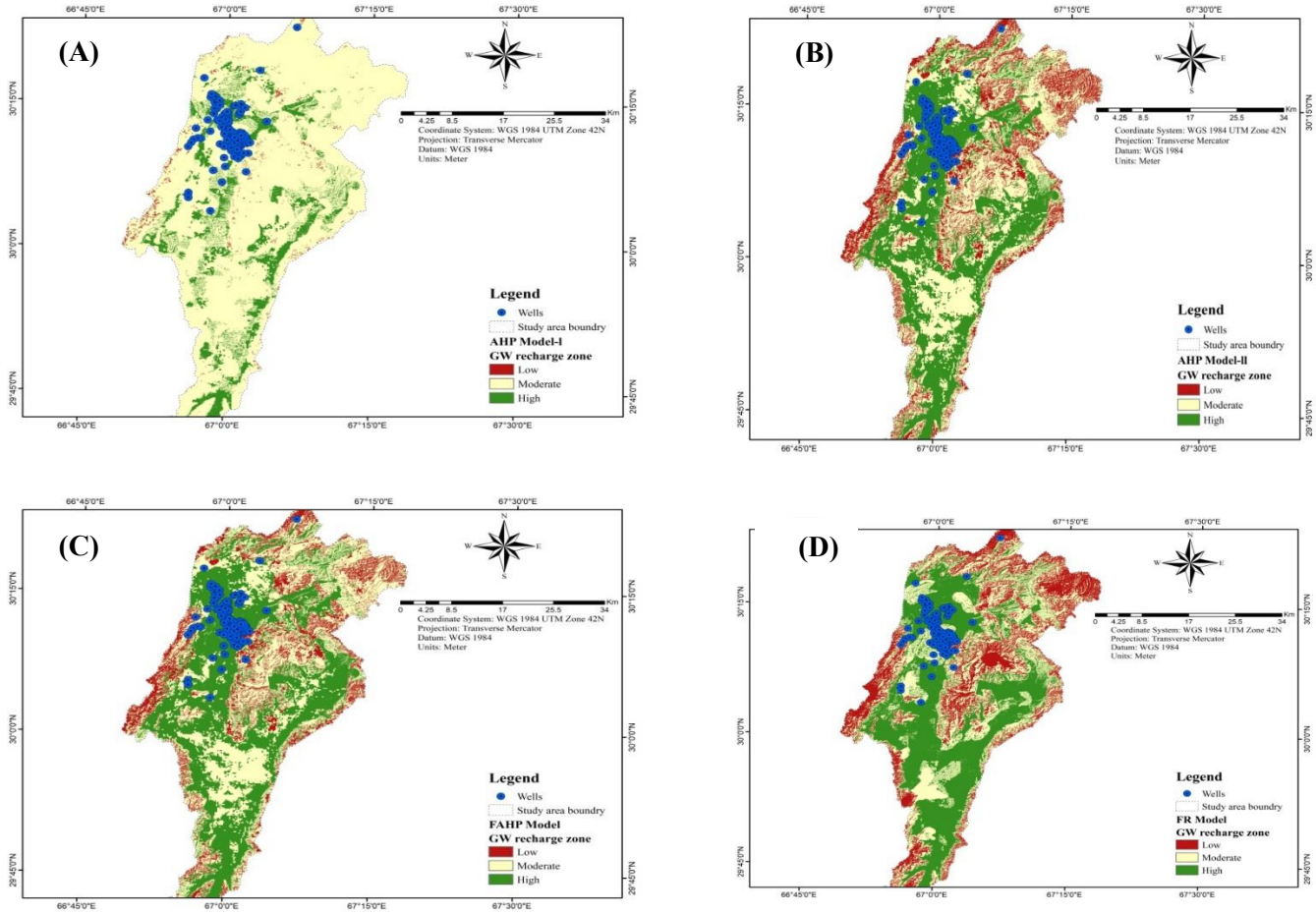

Fig (5): GW recharge zone maps using (A)AHP Model-l(WLC) (B)AHPModel-ll(Wsum) (C)FAHP Model (D)FR Model

Models validation

The Receiver operating characteristic curve (ROC) and area under the curve (AUC) are used to predict classification accuracy (Boughariou et al., 2021; Razandi et al., 2015). Many of the researchers (Arshad et al., 2020a; Elvis et al., 2022; Githinji et al., 2022; Razandi et al., 2015; Tiwari et al., 2017) have used ROC for validation of their research. In the current study, resultant maps of GW recharge potential zone, developed by GIS-based models (AHP, FAHP, FR) have been validated through the ROC curve. AHP model-l, AHP model-ll, FAHP, and FR models showed 84%, 89%, 88%, and 81% prediction accuracy respectively (Fig, 6). Since all these results fall in (0.8-0.9) very good class (Yesilnacar & Topal, 2005),hence applications of all models (AHP, FAHP, FR) showed very good accuracy in spatial prediction of GW recharge zone mapping, but AHP model-ll showed more effectiveness than FAHP and FR in the current study.For cross-validation electrical Conductivity (EC) was used to verify the GW recharge areas. Many researchers (Githinji et al., 2022; Njumbe et al., 2023; Pourtaghi & Pourghasemi, 2014b; Tiwari et al., 2017)used EC to verify demarcated GW recharge zones. The concentration of salt in GW is measured by EC, which reflects the level of ionic concentration in GW(Tiwari et al., 2017). Based on EC readings, GW can be classified into three types. Type-1 GW has EC less than 1500 µS/cm and is fresh-water with a low concentration of salts. Type-2 GW has EC between 1500-3000 µS/cm, indicating a moderate concentration of salts. Type-3 GW has EC greater than 3000 µS/cm, indicating high salinity(Hem, 1985; Sarath Prasanth et al., 2012). In the current analysis 141 wells data, acquired from the Pakistan Council of Research in Water Resources (PCRWR) report, were used.EC range 300-1401 in study area. Based on EC, wells were divided into two types viz, type-1(EC<=1000) considered as High-moderate GW recharge, and type-ll (EC>1000) were considered as low GW recharge zones.

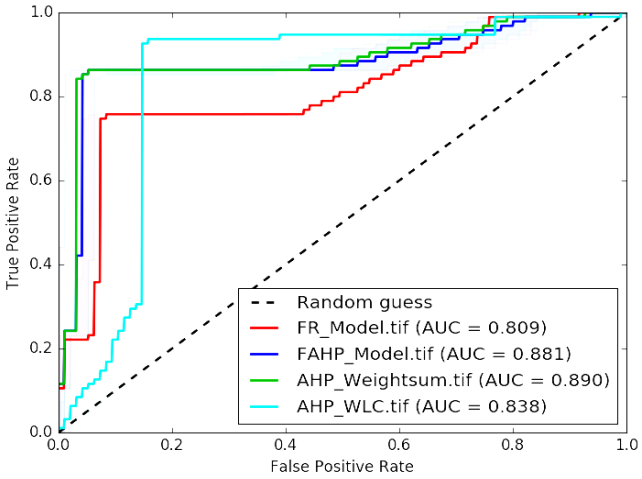

Fig(6): Receiver operating characteristics (ROC) curves for AHP, FAHP and FR models

Based on the outcomes of the Analytic Hierarchy Process (AHP) model-ll, which exhibited a higher accuracy of prediction at 89%, this model was employed for cross-validation, as outlined in Annexure-l-Table.9. The well locations studied were divided into three categories based on their GW (GW) recharge zones: high, moderate, and low. Of the 141 wells surveyed, 119 wells (84%) were located in high GW recharge zones, while 17 wells were in moderate zones and 5 wells were in low recharge zones. In Table.10, the electrical conductivity (EC) of the wells is provided, and it indicates that 98 of the 119 wells (82%) located in high GW recharge zones are in agreement, as well as 13 of the 17 wells (76%) in moderate zones, which fall into type-1 wells. Among the 5 wells classified as type-ll, 3 (60% agreement) are included in this category. Overall, our study demonstrates a high level of agreement (81%) between electrical conductivity and GW recharge.

Conclusions

The study showcases the use of geospatial technology to identify GW recharge potentials in the Quetta region of Pakistan, which is a semiarid-arid area. The study employed AHP, Fuzzy-AHP, and FR models to assign weights to influencing factors and then reclassified selected thematic maps into three classes based on GW recharge zones. Each class was assigned weights based on its significance to GW recharge, and all layers were combined using an AHP-Weighted linear combination, AHP-Weighted sum, fuzzy-AHP overlay, and FR-based models through ArcGIS. The final map resulted in three distinct GW recharge potential zones viz: high, moderate, and low GW recharge zones.

The maps derived from the various models indicate that the central region constitutes the high GW recharge area, while the southern part is characterized by moderate recharge potential. On the other hand, the zones with low recharge potential are located in the mountains, ridges, and residual hills with steeper slopes and higher elevation, where the infiltration capacity is reduced due to high runoff, leading to a decrease in recharge potential. The AHP model-l, AHP model-ll, FAHP model, and FR model demarcated 15%, 39%, 43%, and 42% respectively of an area as high GW recharge The validation of GW recharges potential zones maps, created with GIS-based models (AHP, FAHP, and FR), and was conducted using ROC curves. The accuracy of the predictions made by the AHP model-l, AHP model-ll, FAHP, and FR models were 84%, 89%, 88%, and 81% respectively. These results indicate that the AHP model-ll was the most effective model in this study, outperforming both the FAHP and FR models.These documents will provide a firsthand and valuable guidance to decision-makers in GW resources management and future planning in land use for urban extension especially in water scarce region. This will also help in implementation of future dug/tube wells or boreholes installation in study area which can minimize the cost and effort of hydrogeological investigation.The study area is situated in a remote and mountainous region, which poses a challenge for the availability of well data. The scarcity of well data, in turn, presents a significant obstacle to the development of robust GW modeling and validation.

(Annex-I) Table(9): Accuracy assessment of GWRPZs map with electrical conductivity of GW.

Well No.	Well location		Electrical conductivity (µS/cm)	Well location of GWRZs map	Validation Remarks
	X	Y			
1	308563.156	3340877.000	970	High	Agree
2	307775.166	3340500.220	880	High	Agree
3	308871.500	3340888.000	840	High	Agree
4	309493.000	3338251.000	467	High	Agree
5	307791.737	3341182.345	700	High	Agree
6	307760.940	3341188.381	624	High	Agree
7	309610.000	3337830.000	530	Moderate	Agree
8	308237.757	3341207.013	339	High	Agree
9	309784.814	3340292.468	790	high	Agree
10	308351.883	3340614.400	920	high	Agree
11	309563.568	3339903.804	1080	high	Disagree
12	309661.000	3339781.000	1020	high	Disagree
13	309119.000	3338994.000	1140	high	Disagree
14	308336.000	3339926.000	906	high	Agree
15	308357.593	3340026.000	660	high	Agree
16	308387.000	3339890.000	806	high	Agree
17	308694.765	3338790.898	790	high	Agree
18	309522.448	3340957.000	710	high	Agree
19	307569.603	3340060.000	497	high	Agree
20	308084.000	3339719.000	706	high	Agree
21	308123.000	3340171.000	980	high	Agree
22	309545.289	3340009.100	1184	high	Disagree
23	309545.289	3340009.100	1169	high	Disagree
24	308773.000	3338425.000	690	high	Agree
25	308509.000	3339649.000	670	high	Agree
26	309784.000	3338210.000	1153	high	Disagree
27	309427.650	3338246.109	808	high	Agree
28	308797.269	3340271.800	1280	high	Disagree
29	309108.000	3337984.000	1104	high	Disagree
30	307606.572	3340726.516	1293	high	Disagree
31	308815.907	3339857.828	632	high	Agree
32	307650.958	3340786.330	1104	high	Disagree
33	308526.669	3341385.462	1320	high	Disagree
34	308526.669	3341385.462	1220	high	Disagree
35	309426.000	3338467.000	680	high	Agree
36	308575.934	3340650.413	630	high	Agree
37	308094.000	3338825.000	630	high	Agree
38	307761.000	3339784.000	790	high	Agree
39	308666.915	3341400.250	728	high	Agree
40	307592.864	3339674.378	945	high	Agree
41	307944.000	3341224.000	980	high	Agree
42	309194.000	3339830.000	600	Moderate	Agree
43	308009.279	3339421.000	718	High	Agree
44	310866.389	3338377.250	780	High	Agree

45	308589.000	3340371.000	798	High	
46	309891.965	3342260.664	1134	High	
47	308277.652	3342485.620	926	High	Disagree
48	307889.722	3342028.331	830	High	Agree
49	310561.682	3341355.000	728	High	Agree
50	310932.837	3340538.480	790	High	Agree
51	309221.000	3341707.000	1103	High	Agree
52	310601.652	3340258.691	790	Moderate	Disagree
53	308389.202	3341634.000	1069	High	Agree
54	309165.915	3340800.827	980	High	Disagree
55	309500.756	3342404.540	1016	High	Agree
56	310965.344	3340430.814	530	High	Partially
57	309917.932	3341007.510	709	High	Agree
58	309688.856	3342063.989	820	High	Agree
59	310300.683	3341059.563	448	High	Agree
60	310384.670	3341434.900	906	High	Agree
61	308618.691	3341387.130	1133	High	Agree
62	309725.864	3342320.450	870	High	Disagree
63	309824.372	3342002.303	1214	High	Agree
64	310247.406	3341869.866	1094	High	Disagree
65	311172.660	3340435.700	950	Low	Disagree
66	309709.803	3341783.957	908	High	Agree
67	308644.404	3337722.015	482	Moderate	Agree
68	307029.000	3335841.000	980	High	Agree
69	308559.000	3337729.000	1130	Moderate	Agree
70	306184.420	3340152.147	848	High	Disagree
71	310507.000	3334837.000	1401	Moderate	Agree
72	309198.000	3337346.000	970	High	Disagree
73	306512.774	3332866.735	486	High	Agree
74	309198.000	3337346.000	1121	High	Agree
75	305722.815	3344710.689	880	High	Disagree
76	306928.000	3342211.000	670	High	Agree
77	307169.780	3343364.000	650	High	Agree
78	307619.003	3344827.120	880	High	Agree
79	307479.318	3345461.204	800	High	Agree
80	307283.511	3342152.203	470	High	Agree
81	307246.000	3342133.000	403	High	Agree
82	307201.717	3342022.078	540	High	Agree
83	307013.163	3342004.202	978	High	Agree
84	307331.839	3343607.303	300	High	Agree
85	307687.364	3343051.560	510	High	Agree
86	307192.702	3345739.558	597	High	Agree
87	307192.702	3345739.558	690	High	Agree
88	306992.000	3345961.000	760	High	Agree
89	307035.000	3343162.000	761	High	Agree
90	305636.515	3346935.233	372	High	Agree
91	307495.709	3344417.919	821	High	Agree
92	307655.437	3344507.430	672	High	Agree

93	307860.000	3342880.000	501	High	Agree
94	305293.921	3348142.424	796	High	Agree
95	306711.126	3343950.735	975	High	Agree
96	306545.000	3345344.000	393	High	Agree
97	305182.201	3345967.539	925	High	Agree
98	306910.000	3342089.000	433	High	Agree
99	305285.000	3346953.000	697	High	Disagree
100	304564.000	3342605.000	1238	Moderate	Disagree
101	306456.139	3343395.200	1120	High	Agree
102	306131.088	3344573.008	916	High	Agree
103	302188.000	3343194.000	582	High	Agree
104	307113.179	3344902.111	470	High	Agree
105	302984.413	3341208.276	795	High	Agree
106	302527.000	3341332.000	1280	Low	Agree
107	301777.000	3341078.000	1187	Low	Agree
108	301395.000	3340476.000	651	Moderate	Disagree
109	300879.000	3339678.000	471	Low	Agree
110	307373.000	3340935.000	556	High	Agree
111	307440.411	3345881.936	832	High	Agree
112	308527.284	3347387.985	508	High	Agree
113	303577.764	3352820.245	1003	Moderate	Agree
114	304641.465	3349116.193	489	High	Agree
115	304641.465	3349116.193	580	High	Agree
116	304641.465	3349116.193	458	High	Agree
117	305040.000	3335108.000	928	Moderate	Agree
118	305922.000	3348580.000	865	High	Agree
119	308775.629	3347561.232	556	Moderate	Agree
120	305526.326	3349237.237	513	High	Agree
121	306152.000	3348500.000	489	High	Disagree
122	307582.359	3346108.920	1098	High	Agree
123	309683.262	3347829.949	584	Moderate	Disagree
124	304131.511	3344777.615	1117	Moderate	Agree
125	310216.000	3347108.000	580	Moderate	Agree
126	304775.468	3349752.496	487	High	Agree
127	307377.030	3346341.032	936	High	Agree
128	309367.000	3345719.000	441	High	Agree
129	309506.990	3346265.253	571	Moderate	Agree
130	309618.409	3346345.536	470	High	Agree
131	310341.000	3347096.000	546	Moderate	Agree
132	306849.000	3337545.000	728	High	Agree
133	309020.610	3339120.136	792	High	Agree
134	300828.433	3330412.920	792	High	Agree
135	300912.930	3330906.907	792	High	Disagree
136	306859.000	3339692.000	1195	High	Agree
137	300902.000	3329911.000	511	High	Agree
138	312889.000	3354248.000	490	High	Disagree
139	319012.000	3362469.000	548	Low	Agree
140	313978.000	3344466.000	797	High	Agree
141	304565.000	3327386.000	780	High	Agree

References

Adiat, K., Nawawi, M., & Abdullah, K. (2012). Assessing the accuracy of GIS-based elementary multi criteria decision analysis as a spatial prediction tool–a case of predicting potential zones of sustainable groundwater resources. *Journal of hydrology, 440* ,89-95 .

Aher, P. D., Adinarayana, J., Gorantiwar, S. D., & Sawant, S. A. (2014). Information System for Integrated Watershed Management Using Remote Sensing and GIS. 17-34. doi:10.1007/978-3-319-05906-8_2

Ahmed, A. A., & Shabana, A. R. (2020). Integrating of remote sensing, GIS and geophysical data for recharge potentiality evaluation in Wadi El Tarfa, eastern desert, Egypt. *Journal of African Earth Sciences, 172*, 103957 .

Ahmed, R., & Sajjad, H. (2018). Analyzing factors of groundwater potential and its relation with population in the Lower Barpani Watershed, Assam, India. *Natural Resources Research, 27*(4), 503-515 .

Alam, F., Azmat, M., Zarin, R., Ahmad, S., Raziq, A., Vincent Young, H.-W., . . . Liou, Y.-A. (2022). Identification of Potential Natural Aquifer Recharge Sites in Islamabad, Pakistan, by Integrating GIS and RS Techniques. *Remote Sensing*. doi:10.3390/rs14236051

Ali, I., & Aftab, S. M. (2022). Climate Change and Human-Induced Factor Impacts on Quetta Valley Aquifer, Baluchistan, Pakistan. *Journal of Himalayan Earth Sciences, 55*(2), 21-45 .

Allafta, H., Opp, C., & Patra, S. (2021). Identification of Groundwater Potential Zones Using RemoteSensing and GIS Techniques: A Case Study of the Shatt Al-Arab Basin. *Remote Sensing, 13*, 112 . doi:10.3390/rs13010112

Anbazhagan, S., Ramasamy, S., & Das Gupta, S. (2005). Remote sensing and GIS for artificial recharge study, runoff estimation and planning in Ayyar basin, Tamil Nadu, India. *Environmental geology, 48*, 158-170 .

Aouragh, M. H., Essahlaoui, A., El Ouali, A., El Hmaidi, A., & Kamel, S. (2017). Groundwater potential of Middle Atlas plateaus, Morocco, using fuzzy logic approach, GIS and remote sensing. *Geomatics, Natural Hazards and Risk, 8*(2), 194-206 .

Argaz, A., Ouahman, B., Darkaoui ,A., Bikhtar, H., Yabsa, K., & Laghzal, A. (2019). Application of Remote Sensing Techniques and GIS-Multicriteria decision Analysis for Groundwater Potential Mapping in Souss Watershed, Morocco. *Environmental Sciences, 10*(5), 411-421 .

Arshad, A., Zhang ,Z., Zhang, W., & Dilawar, A. (2020a). Mapping favorable groundwater potential recharge zones using a GIS-based analytical hierarchical process and probability frequency ratio model: A case study from an agro-urban region of Pakistan. *Geoscience Frontiers* .۱۸۱۹-۱۸۰۵ ,(۵)۱۱ ,

Arshad, A., Zhang, Z., Zhang, W., & Dilawar, A. (2020b). Mapping favorable groundwater potential recharge zones using a GIS-based analytical hierarchical process and probability frequency ratio model: A case study from an agro-urban region of Pakistan. *Geoscience Frontiers*. doi:10.1016/j.gsf.2019.12.013

Arulbalaji, P., Padmalal, D., & Sreelash, K. (2019). GIS and AHP techniques based delineation of groundwater potential zones: a case study from southern Western Ghats, India. *Scientific reports, 9*(1), 2082 .

Ashraf, M., & Routray, J. K. (2015). Spatio-temporal characteristics of precipitation and drought in Balochistan Province, Pakistan. *Natural Hazards, 77*, 229-254 .

Ashraf, M., Routray, J. K., & Saeed, M. (2014). Determinants of farmers' choice of coping and adaptation measures to the drought hazard in northwest Balochistan, Pakistan. *Natural Hazards, 73*, 1451-1473 .

Bayati khatibi ,M.,Rostami,F.,Valizadeh Kamran,K.(2022).Investigation and Assessment of Groundwater Vulnerability to Pollution using DRASTIC Model and Fuzzy Logic,Hydrogeomorphology,8(29),81-108.

Boughariou, E., Allouche, N., Ben Brahim, F., Nasri, G., & Bouri, S. (2021). Delineation of groundwater potentials of Sfax region, Tunisia, using fuzzy analytical hierarchy process, frequency ratio, and weights of evidence models. *Environment, Development and Sustainability, 23*(10), 14749-14774 .

Brady, N. C., Weil, R. R., & Weil, R. R. (2008). *The nature and properties of soils* (Vol. 13): Prentice Hall Upper Saddle River, NJ.

Brunelli, M. (2014). *Introduction to the analytic hierarchy process*: Springer.

Buckley, J. J. (1985). Fuzzy hierarchical analysis. *Fuzzy sets and systems, 17*(3), 233-247 .

Carlston, C. (2018). Drainage density and streamflow. Geological Survey Professional Paper 422-C.

Chandra, S. (2006). Contribution of geophysical properties in estimating hydrogeological parameters of an aquifer. *Ph. D. Thesis. BHU, Varanasi*, 176 .

Chandramohan, R., Kanchanabhan, T. E., & Siva Vignesh, N. (2019). Identification of Artificial Recharges Structures Using Remote Sensing and GIS for Arid and Semi-arid Areas. *Nature Environment and Pollution Technology*, 183-189 .

Chaplot, V., & Le Bissonnais, Y. (2000). Field measurements of interrill erosion under different slopes and plot sizes. *Earth Surface Processes and Landforms: The Journal of the British Geomorphological Research Group, 25*(2), 145-153 .

Chen, W., Li, H., Hou, E., Wang, S., Wang, G., Panahi, M . . . ,.Niu, C. (2018). GIS-based groundwater potential analysis using novel ensemble weights-of-evidence with logistic regression and functional tree models. *Science of The Total Environment, 634*, 853-867 .

Chowdhury, A., Jha, M. K., & Chowdary, V. (2010). Delineation of groundwater recharge zones and identification of artificial recharge sites in West Medinipur district, West Bengal, using RS, GIS and MCDM techniques. *Environmental Earth Sciences, 59*, 1209-1222 .

Dabral, S., Bhatt, B., Joshi, J. P., & Sharma ,N. (2014). Groundwater suitability recharge zones modelling – A GIS application. *The International Archives of the Photogrammetry, Remote Sensing and Spatial Information Sciences, XL-8*, 347-353. doi:10.5194/isprsarchives-XL-8-347-2014

Das, S. (2019). Comparison among influencing factor, frequency ratio, and analytical hierarchy process techniques for groundwater potential zonation in Vaitarna basin, Maharashtra, India. *Groundwater for Sustainable Development, 8*, 617-629 .

De Wit, P., & Nachtergaele, F.(1990) .Explanatory note on the soil map of the Republic of Botswana. Annex 1: Typifying pedons and soil analytical data .

Dini.M,Mohammadi,A.(2018).The Zoning of Groundwater Level in the Marand Plain Based on the Existing Potential. Hydrogeomorphology,5(15),17-35.

El-Sawy, K., Ibrahim, A. M., El-Bastawesy, M. A., & El-Saud, W. A. (2016). Automated, manual lineaments extraction and geospatial analysis for Cairo-Suez district (Northeastern Cairo-Egypt), using remote sensing and GIS. *International Journal of Innovative Science, Engineering & Technology, 3*(5), 491-500 .

Elvis, B. W. W., Arsene, M., Theophile, N. M., Bruno, K. M. E., & Olivier, O. A .(۲۰۲۲) .Integration of shannon entropy (SE), frequency ratio (FR) and analytical hierarchy process (AHP) in GIS for suitable groundwater potential zones targeting in the Yoyo river basin, Méiganga area, Adamawa Cameroon. *Journal of Hydrology: Regional Studies, 39*, 100997 .

Essig, E. T., Corradini, C., Morbidelli, R., & Govindaraju, R. S. (2009). Infiltration and deep flow over sloping surfaces: Comparison of numerical and experimental results. *Journal of hydrology, 374*(1-2), 30-42 .

Faust, N., Anderson ,W., & Star, J. (1991). Geographic information systems and remote sensing future computing environment. *Photogrammetric Engineering and Remote Sensing, 57*(6), 655-668 .

Ffolliott, P. F., Baker, M. B., Edminster, C. B., Dillon, M. C., & Mora, K. L. (2012 .(*Land stewardship through watershed management: perspectives for the 21st century*: Springer Science & Business Media.

FitzPatrick, E. A. (1978). An introduction to soil science. *Soil Science, 125*(4), 271 .

Freeze, R. A. (1984). Groundwater contamination: Wiley Online Library.

Gebreyohannes, T., De Smedt, F., Walraevens, K., Gebresilassie, S., Hussien, A., Hagos, M., . . . Gebrehiwot, K. (2017). Regional groundwater flow modeling of the Geba basin, northern Ethiopia. *Hydrogeology Journal, 25*(3), 639 .

Gebrie, T., Gadissa, E., Ahmad, I., Dar, M. A., Teka, A. H., Tolosa, A. T., . . . Fenta, A. (2018). Groundwater resources evaluation using geospatial technology. *Environmental Geosciences, 25*(1), 25-35 .

Githinji, T. W., Dindi, E. W., Kuria, Z. N., & Olago, D .O. (2022). Application of analytical hierarchy process and integrated fuzzy-analytical hierarchy process for mapping potential groundwater recharge zone using GIS in the arid areas of Ewaso Ng'iro–Lagh Dera Basin, Kenya. *HydroResearch, 5*, 22-34 .

Harinarayana, P., Gopalakrishna, G., & Balasubramanian, A. (2000). Remote sensing data for groundwater development and management in Keralapura watersheds of Cauvery basin, Karnataka, India. *Indian Mineral, 34*(2), 11-17 .

Hayat, S., Szabó, Z., Tótha, Á., & Szőnyia, J. M. (2021). MAR site suitability mapping for arid–semiarid regions by remote data and combined. *Acque Sotterranee - Italian Journal of Groundwater,, 10*(3), 17-28. doi:10.7343/as-2021-526as-2021-505

Hem, J. D. (1985). *Study and interpretation of the chemical characteristics of natural water* (Vol. 2254): Department of the Interior, US Geological Survey.

Israil, M., Al-Hadithi, M., & Singhal, D. (2006). Application of a resistivity survey and geographical information system (GIS) analysis for hydrogeological zoning of a piedmont area, Himalayan foothill region, India. *Hydrogeology Journal, 14*(5), 753-759 .

Jerbi, H., Massuel, S., Leduc, C., & Tarhouni, J. (2018). Assessing groundwater storage in the Kairouan plain aquifer using a 3D lithology model (Central Tunisia). *Arabian Journal of Geosciences, 11*, 1-10 .

Kabeto, J., Adeba, D., Regasa, M. S., & Leta, M. K. (2022). Groundwater Potential Assessment Using GIS and Remote Sensing Techniques: Case Study ofWest Arsi Zone, Ethiopia. *Water, 14*. doi:10.3390/w14121838

Khan, A., Govil, H., Taloor, A. K., & Kumar, G. (2020). Identification of artificial groundwater recharge sites in parts of Yamuna River basin India based on Remote Sensing and Geographical Information System. *Groundwater for Sustainable Development, 11*, 100415 .

Khan, A. S., & Khan, S. D. (2013). Land subsidence and declining water resources in Quetta Valley, Pakistan. *Environmental Earth Sciences, 70*(6), 2719-2727. doi:10.1007/s12665-013-2328-9

Khan, A. S ,.Khan, S. D., & Kakar, D. M. (2013). Land subsidence and declining water resources in Quetta Valley, Pakistan. *Environmental Earth Sciences, 70*(6), 2719-2727 .

Kotchoni, D. V., Vouillamoz, J.-M., Lawson, F. M., Adjomayi, P., Boukari, M., & Taylor, R. G .(٢٠١٨) . Relationships between rainfall and groundwater recharge in seasonally humid Benin: a comparative analysis of long-term hydrographs in sedimentary and crystalline aquifers. *Hydrogeology Journal* .

Liu, J., Gao, G., Wang, S., Jiao, L., Wu, X., & Fu ,B. (2018). The effects of vegetation on runoff and soil loss: Multidimensional structure analysis and scale characteristics. *Journal of Geographical Sciences, 28*, 59-78 .

Ma, Y. (2004). GIS Application In Watershed Management. *Nature and Science, 2*(2 .(

Magesh, N. S., Chandrasekar, N., & Soundranayagam, J. P. (2012). Delineation of groundwater potential zones in Theni district, Tamil Nadu, using remote sensing, GIS and MIF techniques. *Geoscience Frontiers, 3*(2), 189-196 .

Mahalingam, B., & Vinay, M. (201 .(٥Identification of ground water potential zones using GIS and Remote Sensing Techniques: A case study of Mysore taluk-Karnataka. *International journal of Geomatics and Geosciences, 5*(3), 393-403 .

Maidment, D. R. (1993). *Handbook of hydrology*: McGraw-Hill.

Malczewski, J. (1999). *GIS and multicriteria decision analysis*: John Wiley & Sons.

Mallick, J., Khan, R. A., Ahmed, M., Alqadhi, S. D., Alsubih, M., Falqi, I., & Hasan, M. A. (2019). Modeling groundwater potential zone in a semi-arid region of Aseer using fuzzy-AHP and geoinformation techniques. *Water, 11*(12), 2656 .

Manap, M. A., Nampak, H., Pradhan, B., Lee, S., Sulaiman, W. N. A., & Ramli, M. F. (2014). Application of probabilistic-based frequency ratio model in groundwater potential mapping using remote sensing data and GIS. *Arabian Journal of Geosciences, 7*, 711-724 .

Maqsoom, A., Aslam, B., Khalid, N., Ullah, F., Anysz, H., Almaliki, A. H., . . . Hussein, E. E. (2022). Delineating Groundwater Recharge Potential through Remote Sensing and Geographical Information Systems. *Water, 14*(11), 1824. doi:10.3390/w14111824

Miller, G. T., & Spoolman, S. E. (2007). *Living in the environment: principles, connections, and solutions.* (16 ed.): Thomson Brooks/Cole.

Moghaddam, D. D., Rezaei, M., Pourghasemi, H ,.Pourtaghie, Z., & Pradhan, B. (2015). Groundwater spring potential mapping using bivariate statistical model and GIS in the Taleghan watershed, Iran. *Arabian Journal of Geosciences, 8*, 913-929 .

Mondal, P., & Dalai, A. K. (2017). *Sustainable utilization of natural resources*: CRC Press.

Nampak, H., Pradhan, B., & Abd Manap, M. (2014). Application of GIS based data driven evidential belief function model to predict groundwater potential zonation. *Journal of hydrology, 513*, 283-300 .

Njumbe, L. J. N., Lordon, A. E. D., & Agyingi, C. M. (2023). Determination of Groundwater Potential Zones on the Eastern Slope of Mount Cameroon using Geospatial Techniques and Seismoelectric Method .

Oh, H.-J., Kim, Y.-S., Choi, J.-K., Park, E., & Lee, S. (2011). GIS mapping of regional probabilistic groundwater potential in the area of Pohang City, Korea. *Journal of hydrology, 399*(3-4), 158-172 .

Ozdemir, A. (2011). GIS-based groundwater spring potential mapping in the Sultan Mountains (Konya, Turkey) using frequency ratio ,weights of evidence and logistic regression methods and their comparison. *Journal of hydrology, 411*(3-4), 290-308 .

P.M., D., & R. Dudal. (1989). Lecture notes on the geography, formation, properties and use of major soils of the world

Pourtaghi, Z. S., & Pourghasemi, H. R. (2014a). Avaliação e mapeamento do potencial em nascentes de água subterrânea com base em SIG no município de Birjand, sul da Província de Khorasan, Irão. *Hydrogeology Journal, 22* .٦٦٢-٦٤٣ ,

Pourtaghi, Z. S., & Pourghasemi, H. R. (2014b). GIS-based groundwater spring potential assessment and mapping in the Birjand Township, southern Khorasan Province, Iran. *Hydrogeol J, 22*(3), 643-662 .

Qureshi, A. S. (2020). Groundwater Governance in Pakistan: From Colossal Development to Neglected Management. *Water, 12*(11), 3017. doi:10.3390/w12113017

Raduła, M. W., Szymura, T. H., & Szymura, M. (2018). Topographic wetness index explains soil moisture better than bioindication with Ellenberg's indicator values. *Ecological indicators, 85*, 172-179 .

Razandi, Y., Pourghasemi, H. R., Neisani, N. S., & Rahmati, O. (2015). Application of analytical hierarchy process, frequency ratio, and certainty factor models for groundwater potential mapping using GIS. *Earth Science Informatics, 8*(4), 867-883 .

Saaty, T. L. (1980). The analytical hierarchy process, planning, priority. *Resource allocation. RWS publications, USA* .

Saranya, T., & Saravanan, S. (2020). Groundwater potential zone mapping using analytical hierarchy process (AHP) and GIS for Kancheepuram District, Tamilnadu, India. *Modeling Earth Systems and Environment, 6*(2), 1105-1122 .

Sarath Prasanth, S., Magesh, N., Jitheshlal, K., Chandrasekar, N., & Gangadhar, K. (2012). Evaluation of groundwater quality and its suitability for drinking and agricultural use in the coastal stretch of Alappuzha District, Kerala, India. *Applied Water Science, 2*, 165-175 .

Sardar, H., Akhter, G., Ge, Y., & Ammar Haider, S. (2022). Delineation of potential managed aquifer recharge sites of Kuchlak sub-basin, Balochistan, using remote sensing and GIS. doi:10.3389/fenvs.2022.916504

Selvam, S., Dar, F. A., Magesh, N., Singaraja, C., Venkatramanan, S., & Chung, S. (2016). Application of remote sensing and GIS for delineating groundwater recharge potential zones of Kovilpatti Municipality, Tamil Nadu using IF technique. *Earth Science Informatics, 9*, 137-150 .

Selvam, S., Manimaran, G., Sivasubramanian, P., & Seshunarayana, T. (2014). Geoenvironmental Resource Assessment Using Remote Sensing and GIS: A case study from southern coastal region. *Research Journal of Recent Sciences, 2277*, 2502 .

Senthilkumar, M., Gnanasundar, D., & Arumugam, R. (2019). Identifying groundwater recharge zones using remote sensing & GIS techniques in Amaravathi aquifer system, Tamil Nadu, South India. *Sustainable Environment Research, 29*(1), 1-9 .

Shaban, A., Khawlie, M., & Abdallah, C. (2006). Use of remote sensing and GIS to determine recharge potential zones: the case of Occidental Lebanon. *Hydrogeology Journal, 14*, 433-443 .

Simmers, I. (1990). Aridity, groundwater recharge and water resources management. *Groundwater recharge. A guide to understanding the natural recharge. Hannover: Ed. R. van Acken GmbH*, 1-20 .

Singh, A., Panda, S., Kumar, K & ,.Sharma, C. S. (2013). Artificial groundwater recharge zones mapping using remote sensing and GIS: a case study in Indian Punjab. *Environmental management, 52*, 61-71 .

Srivastava, P. K., & Bhattacharya, A. K. (2006). Groundwater assessment through an integrated approach using remote sensing, GIS and resistivity techniques: a case study from a hard rock terrain. *International Journal of Remote Sensing, 27*(20), 4599-4620 .

Thakur, D., Bartarya, S. K., & Nainwal, H. C. (2018). Mapping groundwater prospect zones in an intermontane basin of the Outer Himalaya in India using GIS and remote sensing techniques. *Environmental Earth Sciences, 77* .

Tiwari, A. K., Lavy, M., Amanzio, G., De Maio, M., Singh, P. K., & Mahato, M. K. (2017). Identification of artificial groundwater recharging zone using a GIS-based fuzzy logic approach: a case study in a coal mine area of the Damodar Valley, India. *Applied Water Science, 7*, 4513-4524 .

Todd, D. K., & Mays, L. W. (2004). *Groundwater hydrology*: John Wiley & Sons.

Tolche, A .D. (2021). Groundwater potential mapping using geospatial techniques: a case study of Dhungeta-Ramis sub-basin, Ethiopia. *Geology, Ecology, and Landscapes, 5*(1), 65-80 .

Uc Castillo, J. L., Martínez Cruz, D. A., Ramos Leal , J. A., Tuxpan Vargas, J., Rodríguez Tapia, S. A., & Marín Celestino, A. E. (2022). Delineation of Groundwater Potential Zones (GWPZs) in a Semi-Arid Basin through Remote Sensing, GIS, and AHP Approaches. *Water, 14*. doi:10.3390/w14132138

V.Keshavan, S.Ranjith, J.Sabarish, J.Srinivasan, & D.Sivasankar. (2017). Identification of Groundwater Recharge Potential Zones for a Watershed Using Remote Sensing and GIS. *International Journal of Innovative Research in Science, Engineering and Technology, 16*(4). doi:10.15680/IJIRSET.2017٠٦٠٤٠٤٨.

Watto, M. A. (2015). The economics of groundwater irrigation in the Indus Basin, Pakistan: Tube-well adoption, technical and irrigation water efficiency and optimal allocation. University of Western Australia .

Xu, G., Su, X., Zhang, Y., & You ,B. (2021). Identifying Potential Sites for Artificial Recharge in the Plain Area of the Daqing River Catchment Using GIS-Based Multi-Criteria Analysis. *Sustainabilty, 13*. doi:10.3390/su13073978

Yeh, H.-F., Lee, C.-H., Hsu, K.-C., & Chang, P.-H. (2009). GIS for the assessment of the groundwater recharge potential zone. *Environmental geology, 58*, 185-195 .

Yesilnacar, E., & Topal, T. (2005). Landslide susceptibility mapping: a comparison of logistic regression and neural networks methods in a medium scale study, Hendek region (Turkey). *Engineering Geology, 79*(3-4), 251-266 .

Yıldırım, Ü. (2021). Identification of groundwater potential zones using GIS and multi-criteria decision-making techniques: a case study upper Coruh River basin (NE Turkey). *ISPRS International Journal of Geo-Information, 10*(6), 396 .

Yuan, J., Lei, T., Guo, S., & Jiang, D. (2001). Study on spatial variation of infiltration rates for small watershed in loess plateau. *J. Hydraul. Eng, 10*, 88-92 .

Zadeh, L. A. (1965). Fuzzy sets. *Information and control, 8*(3), 338-353 .

مقاله پژوهشی

بررسی تغذیه آبهای زیرزمینی و مسـّاحی مکان های تغذیه با استفاده از سیستم های تصمیم گیری فضایی یکپارچه مبتنی بر GIS ، مطالعه موردی : از منطقه کویته پاکستان

عماد علی [۱]*،مریم بیاتی خطیبی [۲] ،صدراکریم زاده [۳]

1- دانشجوی دکتری سنجش از دور وسیستم اطلاعات جغرافیایی، دانشکده برنامه ریزی وعلوم محیطی، دانشگاه تبریز، تبریز ، ایران. Imadali_khan@yahoocom

2-استاد گروه سنجش از دور وسیستم اطلاعات جغرافیایی دانشکده برنامه ریزی وعلوم محیطی دانشگاه تبریز،تبریز، ایران. m_bayati@tabrizu.ac.ir

3- استادیارگروه سنجش از دور وسیستم های اطلاعات جغرافیایی دانشکده برنامه ریزی وعلوم محیطی، دانشگاه تبریز،تبریز، ایران. skharimzadeh@tabrizu.ac.ir

کلیدواژه‌ها

منطقه بندی تغذیه آب های زیر زمینی،فرایندتحلیل سلسله مراتبی ،فرایند سلسله مراتب تحلیلی یکپارچه ،نسبت فرکانس ،کویته پاکستان .

چکیده

آب های زیرزمینی یک منبع حیاتی در مناطق خشک و نیمه خشک محسوب می شوند.منطقه کویته پاکستان ازمناطق کمبود آب دنیا به شمار می آیدکه برای مدیریت منابع آب زیرزمینی به مطالعه و مساحی های دقیق نیاز دارد تا محدوده های تغذیه آب های زیر زمینی مشخص گردند. این مطالعه با هدف ترسیم مناطق تغذیه آب های زیرزمینی با استفاده از ترکیبی از مدل‌های فرآیند تحلیل سلسله مراتبی (AHP)، فازی-AHP و نسبت فرکانس (FR) انجام شد. هدف دیگر ،مطالعه مقایسه اثربخشی مدل‌ها در نقشه‌برداری محدوده هایی از منطقه با پتانسیل تغذیه آب زیرزمینی بود. برای دستیابی به این اهداف، ۹ عامل موثر بر آب های زیرزمینی شامل زمین شناسی، انواع خاک، تراکم آبراهه ها، ارتفاع، شیب، شاخص رطوبت توپوگرافی، پوشش اراضی کاربری و بارندگی در نظر گرفته شد. نقشه های موضوعی برای همه عوامل با استفاده از داده های ماهواره ای در محیط ArcGIS تولید شد. وزن هر لایه موضوعی بر اساس اهمیت آن برای تغذیه مجددآبخوان ها تعیین شد. همه لایه‌های موضوعی با استفاده از AHP model-l (WLC)، AHP model-II (جمع وزنی)، پوشش فازی-AHP، و مدل مبتنی بر FR با استفاده از ArcGIS ترکیب شدند. یافته‌ها نشان داد که ۱۵٪ و ۳۹٪ منطقه مورد مطالعه به ترتیب دارای پتانسیل شارژ مجدد بر اساس مدل-I مبتنی بر AHP و مدل-II هستند. مدل FAHP ۴۳درصد از منطقه را به عنوان مناطقی با تغذیه بالا مشخص می کند ،در حالی که مدل FR ۴۲درصد از منطقه را به عنوان مناطقی با تغذیه بالا نشان می دهد. اکثر مناطق با تغذیه آب زیرزمینی بالا در بخش مرکزی منطقه قراردارند، در حالی که بخش جنوبی به عنوان یک منطقه با تغذیه متوسط و قسمت های شرقی و غربی به عنوان مناطق با پتانسیل تغذیه کم مشخص شده اند. برای تأیید صحت این مدل‌ها، از منحنی‌های اعتبارسنجی مشخصه عملکرد گیرنده (ROC) استفاده شد. منحنی‌های ROC نشان داد که مدل AHP-II دارای بالاترین دقت (AUC=89%) است در حالی که مدل FAHP (88=AUC=%)، AHP model-I (AUC=84%) و FR (AUC=81%) درمرحله بعدی قراردارند. در نتیجه، مدل AHP-II در مقایسه با مدل‌های FAHP و FR در مطالعه حاضر در تعیین محدوده منطقه شارژ مؤثرتر نشان داده شد.

تاریخ دریافت: ۱۴۰۳/۰۲/۰۱

تاریخ پذیرش: ۱۴۰۳/۰۴/۰۴

تاریخ انتشار: ۱۴۰۳/۰7/30

نویسنده مسئول: عماد علی

رایانامه: E-mail:Imadali_khan@yahoo.com

ارجاع به این مقاله: عماد؛ علی، مریم، بیاتی خطیبی، صدرا؛ کریم زاده(.۱۴۰۳). بررسی تغذیه ی آب های زیرزمینی ومساحی مکان های تغذیه با استفاده از سیستم های تصمیم گیری فضایی یک پارچه مبتنی برGIS، مطالعه موردی: از منطقه کویته پاکستان. هیدروژئومورفولوژی ۱۱(۴۰):۸۶-۵۸.

DOI:10.22034/hyd.2024.61290.1734

Publisher: University of Tabriz